RESEARCH ACTIVITIES IV
Department of Molecular Assemblies

IV-A Spectroscopic Study of Organic Conductors

The reflectivity of an organic conductor provides us with a wealth of information on the electronic structure. For instance, the anisotropy of a band structure, bandwidth, effect of electron-electron correlation, and electron-molecular vibration (EMV) coupling parameters can be extracted from the analysis of the reflectivity or optical conductivity curve. We are investigating the polarized reflection spectra of various organic conductors in the spectral region of 50–33000 cm^{-1} and in the temperature range of 6–300 K. Raman spectroscopy is a complementary method to reflection spectroscopy for understanding molecular vibrations (local phonons). We are investigating the charge ordering (CO) or charge disproportionation phenomena in organic conductors using the technique of vibrational spectroscopy. The charge ordering was found in inorganic narrow-band systems such as copper, manganese, and vanadium oxides. Recently, a charge-ordered ground state has been found in several organic conductors. The Raman and infrared spectra change dramatically at CO phase-transition temperature. Our goal is the complete understanding of the CO phase transition through the interpretation of the vibrational spectra, and the drawing of a P-T phase diagram using Raman spectra.

IV-A-1 Charge Ordering in θ-(BEDT-TTF)$_2$RbZn(SCN)$_4$ Studied by Vibrational Spectroscopy

YAMAMOTO, Kaoru; YAKUSHI, Kyuya; MIYAGAWA, Kazuya[1]; KANODA, Kazushi[1]; KAWAMOTO, Atsushi[2]
([1]Univ. Tokyo; [2]Hokkaido Univ.)

[*Phys. Rev. B* submitted]

Spatial charge distribution in an insulating phase of θ-(BEDT-TTF)$_2$RbZn(SCN)$_4$ was investigated using polarized Raman and infrared (IR) spectroscopy. Figure 1 shows polarized Raman and IR spectra of the natural (non-substituted) and ^{13}C-substituted samples in the insulating phase. Both the Raman and IR spectra showed a complicated multiple-peak pattern stemming from two modes based on ring (ν_2) and central C=C stretchings (ν_3). From the isotope-shifts, we attributed peaks **a$_1$** and **a$_2$** to ν_2 and peaks **b$_1$**, **b$_2$**, **c$_1$**, and **c$_2$** to ν_3. While it is known that ν_2 and ν_3 commonly show a large frequency shift in proportion to a variation in the molecular charge, ν_3 provides a larger vibronic coupling effect than ν_2. Because of the strong vibronic-coupling, ν_3-related peaks showed a large Davydov splitting, allowing us to perform factor group analysis to specify the spatial pattern of the charge distribution. Meanwhile, the strong vibronic coupling causes an irregular frequency shift, hindering us to calculate the charge-disproportionation (CD) ratio from the frequency. To avoid the complicated shift due to the vibronic coupling, we used the weakly coupled mode ν_2 for the estimation of the CD ratio. The calculated ratio agrees with the value estimated by an NMR study. The agreement of the conclusions drawn by the two different approaches substantiates the explanation for the charge distribution and the reliability of this estimation method.

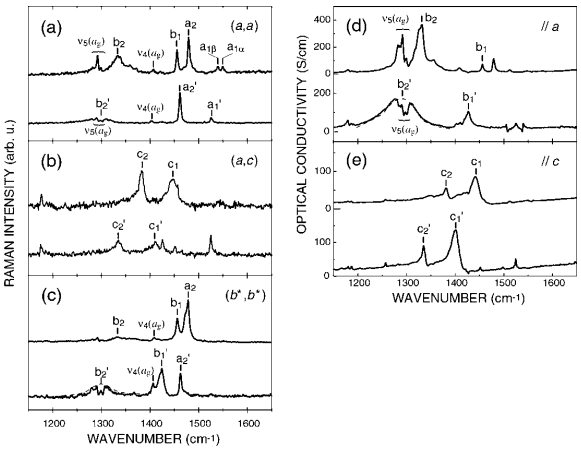

Figure 1. Polarized Raman and optical conductivity spectra of the natural (upper curve) and ^{13}C-substituted (lower curve) θ-(BEDT-TTF)$_2$RbZn(SCN)$_4$. (a), (b), and (c) show the (*a*,*a*), (*a*,*c*), and (*b**,*b**)-polarized Raman spectra, and (d) and (e) show the *a*- and *c*-polarized optical conductivity spectra, respectively. (*T* = 50 K)

IV-A-2 Charge Disproportionation Ratio of (BEDT-TTF)$_3$CuBr$_4$ Studied by a Molecular Vibration Frequency

YAMAMOTO, Kaoru; YAKUSHI, Kyuya; YAMAURA, Jun-ichi[1]; ENOKI, Toshiaki[2]
([1]Inst. Solid State Phys.; [2]Tokyo Inst. Tech.)

Vibrational spectroscopy is a powerful tool to investigate charge distribution in charge transfer salts. Based on Raman and IR measurements for θ-(ET)$_2$RbZn(SCN)$_4$, (ET: BEDT-TTF) we have proposed that a molecular charge can be estimated from the frequency of the ring C=C stretching mode (ν_2). In order to verify the reliability of the argument, we applied this analysis to other ET salts with a different molecular arrangement and band filling from the θ-type salt. The title compound (ET)$_3$CuBr$_4$ has a 3:1 stoichiometry. According to the x-ray diffraction study, the semi-

conductive salt shows charge ordering from room temperature. Raman spectra of this salt showed multiple peaks in the C=C stretching region. Based on the polarization dependence, we found two ν_2-related peaks among the multiple peaks. Figure 1 shows the reported ν_2 frequencies plotted with respect to the molecular charge. According to this plot, the observed two peaks are positioned approximately at +0.9*e* and +0.2*e*. Supposing that there are two differently charged ET molecules (+0.9*e* and +0.2*e*) in the ratio of 2:1, the average molecular charge is consistent with the stoichiometry. This suggests the certainty of the interpretation. This result supports the conclusion of the x-ray study proposing the presence of charge ordering, and demonstrates that the molecular-charge-estimation based on the ν_2 frequency can be applied for various systems.

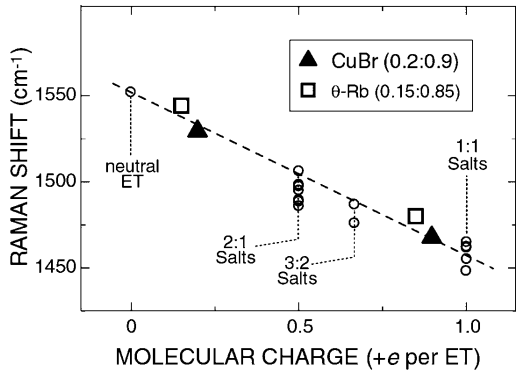

Figure 1. Raman frequencies of the ring C=C stretching (ν_2) modes *vs.* molecular charge.

IV-A-3 Charge and Molecular Arrangement in (DI-DCNQI)$_2$Ag Studied by Vibrational Spectroscopy

YAMAMOTO, Kaoru; YAKUSHI, Kyuya; HIRAKI, Koichi[1]; TAKAHASHI, Toshihiro[1]; KANODA, Kazushi[2]; MENEGHETTI, Moreno[3]
([1]Gakushuin Univ.; [2]Univ. Tokyo; [3]Univ. Padova, Italy)

(DI-DCNQI)$_2$Ag (see the inset of Figure 1) has a one-dimensional (1D) structure with a quarter-filled band. An x-ray diffraction and NMR studies revealed that there was a $4k_F$ charge-density wave (CDW) below 220 K. Both studies claim the $4k_F$ site CDW (see Figure 1c) for the insulating state of this compound. To examine the possible $4k_F$ bond CDW (see Figure 1d), we studied the molecular vibrations, since the vibronic modes are extremely sensitive to the lattice modulation such as bond CDW. As shown in Figure 1a, the optical conductivity spectrum of (DI-DCNQI)$_2$Ag shows clear vibronic bands below 3000 cm^{-1}, in contrast to (DMe-DCNQI)$_2$Cu, which is metallic with a uniform stacking structure. Because the CT dipole moments induced by EMV coupling are cancelled out in a uniform stack (1b) and $4k_F$ site CDW (1c) as shown in Figure 1, the appearance of the vibronic bands strongly suggests the $4k_F$ bond CDW (1d). Low-temperature Raman and IR measurements are in progress to examine whether the bond CDW and site CDW coexist or not.

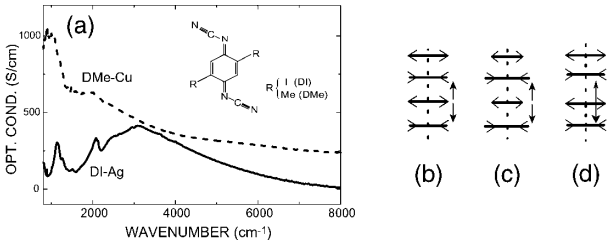

Figure 1. (a) Optical conductivity spectra of (DI-DCNQI)$_2$Ag (solid line) and (DMe-DCNQI)$_2$Cu (dashed line) measured at room temperature. Schematic models of vibronically induced charge-transfer moment in (a) uniformly stacked, (b) $4k_F$ site CDW, and (c) $4k_F$ bond CDW. Horizontal bars and arrows represent a charge density and phase of a molecular vibration, respectively. Perpendicular arrows indicate the CT dipole moments induced by the molecular vibration.

IV-A-4 The C=C Stretching Vibrations of κ-(BEDT-TTF)$_2$Cu[N(CN)$_2$]Br and Its Isotope Analogues

MAKSIMUK, Mikhail[1]; YAKUSHI, Kyuya; TANIGUCHI, Hiromi[2]; KANODA, Kazushi[2]; KAWAMOTO, Atsushi[3]
([1]IMS and Inst. Problem Chem. Phys.; [2]Tokyo Univ.; [3]Hokkaido Univ.)

[*J. Phys. Soc. Jpn.* submitted]

The C=C stretching modes in resonance Raman spectra and infrared reflectivity were measured at temperatures between 15 K and 300 K using various polarizations in κ-(BEDT-TTF)$_2$Cu[N(CN)$_2$]Br, its fully and partially deuterated analogues. The infrared- and Raman-active bands were re-assigned based on the factor group analysis. As shown in Figure 1, we found a Raman-active EMV-coupled ν_3 mode near 1420 cm^{-1}, which has B_{2g} symmetry and shows a large downshift and broadening through the inter-dimer EMV interaction. The ν_2 and ν_3 modes are respectively the ring and bridge C=C stretching vibration, which mix with each other depending upon the positive charge on BEDT-TTF. We found that the mixing of the bridge and ring C=C stretching vibrations depended upon the symmetry of the crystal mode. The ν_{27} mode is an asymmetric ring C=C vibration, which vibrates out-of-phase within a dimer in the ν_{27} (A_g) crystal mode. In contrast to deuterated crystals, the non-deuterated crystals show a splitting in the ν_2, ν_3, and ν_{27}. The origin of this unusual finding is not clear at present.

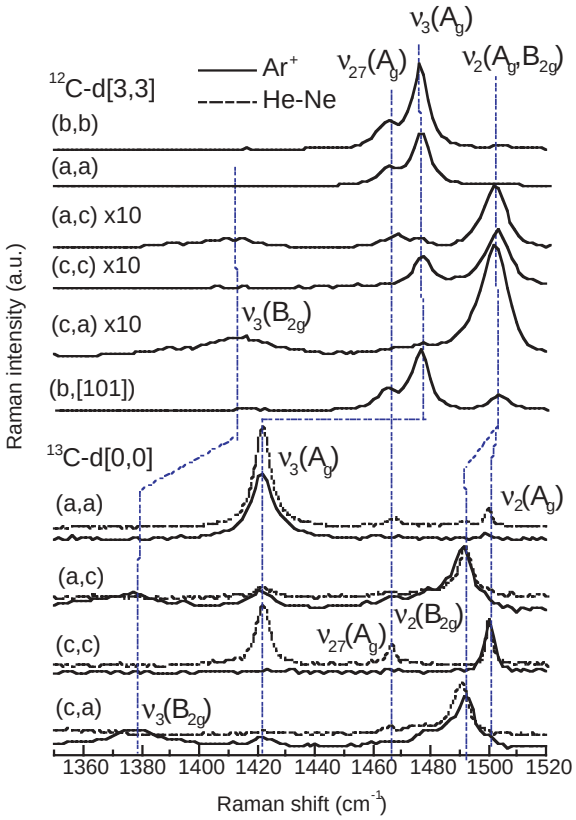

Figure 1. Raman spectra of ^{12}C-d[3,3] and ^{13}C-d[0,0] at 20 K. The intensity among the different polarizations is approximately scaled to each other in ^{12}C-d[3,3], but not scaled in ^{13}C-d[0,0]. In ^{12}C-d[3,3], three hydrogen atoms in each ethylene group are replaced by deuterium, and in ^{13}C-d[0,0], the two central ^{12}C atoms bridging the 1,3-dithiol rings are replaced by the carbon isotope ^{13}C.

IV-A-5 Plasma Frequency and Optical Effective Mass of κ-(ET-d_8)$_2$Cu(CN)[N(CN)$_2$]

DROZDOVA, Olga[1]; YAKUSHI, Kyuya; YAMOCHI, Hideki[2]; SAITO, Gunzi[2]
([1]IMS and Yoffe Inst. Phys., [2]Kyoto Univ.)

κ-(ET)$_2$Cu(CN)[N(CN)$_2$] is a strongly correlated organic metal with superconducting transition at T_C = 11.2 K (ET-h_8) and T_C = 12.3 K (ET-d_8) at ambient pressure. Optical study was undertaken on single crystals of deuterated compound in a wide frequency region from far-IR to UV, along two main directions in the conducting (100) plane, at temperatures down to 6 K.

The tight-binding band calculation at 300 K predicts the intraband transition of the free charge carriers for two upper band branches, with the total calculated plasma frequency ~7000 cm^{-1} and the effective mass m^*/m_e = 2. However, in the experimental reflectivity spectra, the intraband transition appears at much lower frequency (ω < 300 cm^{-1} at T = 300 K). Almost no Drude peak can be found in the optical conductivity, and most of the spectral weight is contained in the broad mid-infrared peak.

Two distinctive temperature regions can be found. From 300 K down to 150 K, intensity of the mid-infrared peak increases together with the intensity of the coupled EMV features. Below 150 K, the far-infrared reflectivity starts to grow rapidly. In the optical conductivity, it is accompanied by the shift of the spectral weight from the mid-infrared peak and EMV coupled features to the Drude peak.

The parameters of the electronic structure (ω_p, Γ_e) were obtained from the Drude-Lorentz dispersion analysis. At lower temperatures, the plasma frequency is rapidly growing (ω_p ~ 5500 cm^{-1} at 6 K). Ordinary sources of the low-temperature increase of the plasma frequency in a metal (Fermi-Dirac function, increase of the transfer integrals due to the crystal shrinking) cannot justify the observed three-to-four-fold growth. However, the growth of the plasma frequency can be explained by a temperature-dependent density of states in the strongly correlated metal accompanying a crossover from an incoherent transport at high temperatures to a coherent regime at lower *T*.

IV-A-6 Charge Order in θ-(BDT-TTP)$_2$Cu(NCS)$_2$

YAKUSHI, Kyuya; OUYANG, Jianyong[1]; SIMONYAN, Mkhitar[2]; MISAKI, Yohji[3]; TANAKA, Kazuyoshi[3]
([1]GUAS; [2]IMS and Inst. Phys. Res. ARAS; [3]Kyoto Univ.)

[*Mol. Cryst. Liq. Cryst.* in press]

θ-(BDT-TTP)$_2$Cu(NCS)$_2$ is a highly correlated organic conductor with a quasi-two-dimensional electronic structure. We have found a charge disproportionation in θ-(BDT-TTP)$_2$Cu(NCS)$_2$ accompanying the phase transition at 250 K.[1)] The magnetic properties of this compound was examined to know the pattern of the ordered charge. The paramagnetic susceptibility conforms to Curie-Weiss law down to about 30 K, makes a peak at 5–10 K, and drops to nearly zero at 1.8 K. This behavior suggests that the exchange interaction between localized charge is much weaker than that of θ-(BEDT-TTF)$_2$RbZn(SCN)$_4$ which shows a similar charge ordering phase transition. This result and the comparison of the optical conductivity with a theoretical calculation strongly suggest that the localized charge forms a vertical stripe in contrast to the horizontal stripe in θ-(BEDT-TTF)$_2$RbZn(SCN)$_4$. The horizontal stripe is more stable than the vertical stripe according to the calculation of Madelung energy in both compounds. The degree of charge disproportionation δ = 0.1–0.2, in (BDT-TTP)$^{\delta+}$(BDT-TTP)$^{(1-\delta)+}$ is also almost the same as that of θ-(BEDT-TTF)$_2$RbZn(SCN)$_4$ (δ = 0.1$_5$). The investigation of the reasoning of the different nature between θ-(BDT-TTP)$_2$Cu(NCS)$_2$ and θ-(BEDT-TTF)$_2$-RbZn(SCN)$_2$ is now in progress.

Reference

1) J. Ouyang, K. Yakushi, Y. Misaki and K. Tanaka, *Phys. Rev. B* **63**, 54301 (2001).

IV-A-7 Assignment of the In-Plane Molecular Vibrations of the Electron-Donor Molecule BDT-TTP Based on Polarized Raman and Infrared Spectra

OUYANG, Jianyong[1]; YAKUSHI, Kyuya; KINOSHITA, Tomoko[1]; NANBU, Shinkoh; AOYAGI, Mutsumi; MISAKI, Yohji[2]; TANAKA, Kazuyoshi[2]
([1]GUAS; [2]Kyoto Univ.)

[*Spectrochim. Acta, Part A* in press]

To interpret the change of the vibrational spectrum accompanying the charge ordering and/or asymmetric charge distribution within the BDT-TTP molecule, we conducted the normal mode analysis of BDT-TTP. We first analyzed TTP-DO which have a TTP skeleton in order to obtain the force constants in the TTP skeleton, and then analyzed BDT-TTP based on the empirical force constants. The vibrational modes of TTP-DO are assigned with the aid of the depolarization ration of solution Raman spectra, polarized reflection and Raman spectra of single crystals. A D_{2h} symmetry is assumed for the BDT-TTP molecule and its in-plane fundamental vibrations are assigned with the aid of the polarization ratio and the correlation with TTP-DO, TTF, TMTTF, and BEDT-TTF. Normal coordinate calculation with a modified internal valence force field was carried out for the in-plane fundamental vibrations of TTP-DO and BDT-TTP. *Ab initio* calculations of the normal modes of BDT-TTP^0 and BDT-TTP$^+$ were compared with the empirical analysis. The agreement with the result of the empirical analysis was very good.

IV-A-8 Spectroscopic Study of the [0110] Charge Ordering in (EDO-TTF)$_2$PF$_6$

DROZDOVA, Olga[1]; YAKUSHI, Kyuya; OTA, Akira[2]; YAMOCHI, Hideki[2]; SAITO, Gunzi[2]
([1]IMS and Yoffe Inst. Phys.; [2]Kyoto Univ.)

(EDO-TTF)$_2$PF$_6$ is a novel organic metal, which undergoes a complex phase transition at 280 K. The feature of the phase transition includes a sharp metal-insulator transition with 1st order canceling of the magnetic moment, order-disorder transformation of PF_6, drastic change in the donor packing and shape, and a charge ordering.

IR spectra at 295 K show the Drude-like reflectivity along the stack (E||*b*), and a low background with a number of phonons for the perpendicular (E||*a**) direction. The optical conductivity for E||*b* displays a peak of 1500 Ω^{-1}cm^{-1} centered at 1200 cm^{-1}, which extrapolates smoothly to the measured conductivity σ_{dc} = 50 Ω^{-1}cm^{-1}. The peak has a distorted shape, with a dip due to the EMV coupling at 1400 cm^{-1}, and an extended high-frequency tail presumably due to the electron correlation effect. The electronic spectrum for E||*b* changes drastically below the phase transition: the peak at 1200 cm^{-1} completely disappears, and instead two charge-transfer bands emerge. The first is of $D^0D^+ \rightarrow D^+D^0$ type, centered at 4500 cm^{-1}. It is the lowest electronic excitation of the low-temperature phase, and it compares well with the energy gap E_g = 0.64 eV measured on the compressed powder pellet. The second band is at 11150 cm^{-1}, corresponding to $D^+D^+ \rightarrow D^{2+}D^0$ charge transfer.

Profound change appears in the vibrational spectra in the region of charge-sensitive C=C stretching modes, as well. Neutral EDO-TTF has three C=C modes: ν_1 (EDO-ring, 1648 cm^{-1}), ν_2 (TTF-ring, 1538 cm^{-1}), and ν_3 (central, 1498 cm^{-1}). In the high-temperature phase, three IR and three Raman active C=C modes are allowed and can be observed in the specific polarizations. Their frequencies correspond to EDO-TTF$^{0.5+}$. Below 280 K, these are split into a total of 12 modes (6 IR + 6 R), half due to the charge-poor EDO-TTF and half due to the charge-rich ones. ν_3 and ν_1 of the charge-rich EDO-TTF were found to be strongly interacting with the 11150 cm^{-1} charge-transfer band, as evidenced by both the IR spectrum along the stacking axis, and by the selective resonance Raman effect of these modes with the 785 nm excitation wavelength in the same direction. From the ionization shifts, it was estimated that the charge on the charge-poor and charge-rich molecules is ≤ +0.1*e* and ≥ +0.9*e*, respectively, *i.e.* the charge is completely separated.

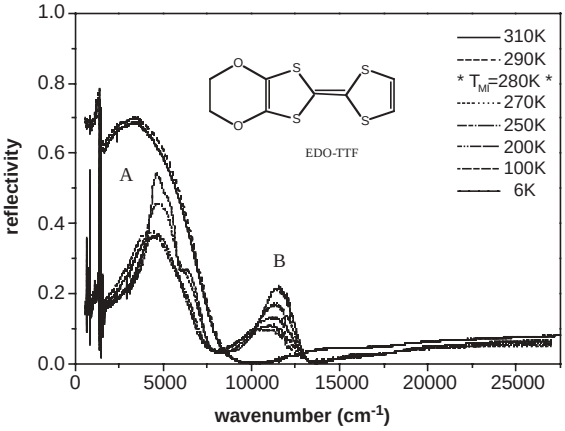

Figure 1. Temperature dependence of the reflection spectrum of EDO-TTF. The spectrum drastically changes from a metallic to insulating reflectivity at the phase transition temperature. The bands A and B correspond to the charge-transfer transitions of $D^+D^0 \rightarrow D^0D^+$ and $D^+D^+ \rightarrow D^0D^{2+}$, which clearly indicate the charge ordering such as $D^0D^+D^+D^0$.

IV-A-9 Structural and Spectroscopic Study of Quasi-One-Dimensional Organic Conductor, (BDTFP)$_2$X(C$_6$H$_5$Cl)$_{0.5}$ (X = AsF$_6$, PF$_6$)

URUICHI, Mikio; YAKUSHI, Kyuya; SHIRAHATA, Takashi[1]; TAKAHASHI, Kazuko[1]; MORI, Takehiko[2]; NAKAMURA, Toshikazu
([1]Tohoku Univ.; [2]Tokyo Inst. Tech.)

In (BDTFP)$_2$X(PhCl)$_{0.5}$ (X = PF_6, AsF_6), the BDTFP molecules are stacked along the *c*-axis with a dimerized structure. The crystal structure and polarized reflection spectra suggest a quasi-1D electronic structure along the *c*-axis. In spite of the isomorphous structure at room temperature, the PF_6 and AsF_6 salts show different kinds of phase transition. (BDTFP)$_2$PF$_6$(PhCl)$_{0.5}$ shows a magnetic phase transition at 175 K accompanying a resistivity jump, and undergoes a non-magnetic ground state. On the other hand, (BDTFP)$_2$AsF$_6$(PhCl)$_{0.5}$ shows a first-order phase transition at 250 K, and undergoes first a paramagnetic state and then an anti-ferromagnetic ground state. We determined the low-temperature

crystal structures below the phase transition temperature. In the former, the *c*-axis was doubled and thus the dimerized structure changed into a tetramerized structure. At the same time, a new charge-transfer transition appeared at 7000~8000 cm^{-1}. These two findings are consistent with the non-magnetic state. In the latter, on the other hand, dimerized structure was maintained below the phase transition temperature, and instead AsF_6 ion rotated with *ca*. 10° rotation of BDTFP. This structural change seems to be the origin of the first-order phase transition to a paramagnetic state.

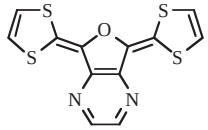

BDTFP

References

1) T. Ise, T. Mori and K. Takahashi, *J. Mater. Chem.* **11**, 264 (2001).
2) T. Nakamura, K. Takahashi, T. Ise, T. Shirahata, M. Uruichi, K. Yakushi and T. Mori, *Mol. Cryst. Liq. Cryst.* in press.

IV-A-10 Crystal Chemistry and Physical Properties of Superconducting and Semiconducting Charge Transfer Salts of the Type (BEDT-TTF)$_4$[$A^{I}M^{III}(C_2O_4)_3$] PhCN (A^{I} = H_3O, NH_4, K; M^{III} = Cr, Fe, Co, Al; BEDT-TTF = Bis(ethylenedithio) tetrathiafulvalene)

MARTIN, Lee[1]; TURNER, Scott T.[1]; DAY, Peter[1]; GUIONNEAU, Philippe[2]; HOWARD, Judith A. K.[3]; HIBBS, Dai E.[4]; LIGHT, Mark E.[4]; HURSTHOUSE, Michel B.[4]; URUICHI, Mikio; YAKUSHI, Kyuya

([1]Royal Inst. GB; [2]Inst. Chim. Matiere Condensee de Bordeaux; [3]Univ. Durham; [4]Univ. Southampton)

[*Inorg. Chem.* **40**, 1363 (2001)]

Synthesis, structure determination by single-crystal X-ray diffraction, and physical properties are reported and compared for superconducing and semiconducting molecular charge-transfer salts with stoichiometry (BEDT-TTF)$_4$[$A^{I}M^{III}(C_2O_4)_3$] PhCN, where A^{I} = H_3O, NH_4, K; M^{III} = Cr, Fe, Co, Al. Attempts to substitute M^{III} with Ti, Ru, Rh, or Gd are also described. New compounds with M = Co and Al are prepared and detailed structural comparisons are made across the whole series. Compounds with A = H_3O^+ and M = Cr, Fe are monoclinic (space group *C2*/*c*), at 150, 120 K *a* = 10.240(1) Å, 10.232(2) Å; *b* = 19.965(1) Å, 20.04(3) Å; *c* = 34.905(1) Å, 34.97(2) Å; β = 93.69(1)°, 93.25(1)°, respectively, both with *Z* = 4. These salts are metallic at room temperature, becoming superconducting at 5.5(5) or 8.5(5) K, respectively. A polymorpoh with A = H_3O^+ and M = Cr is orthorhombic (*Pbcn*) with *a* = 10.371(1) Å, *b* = 19.518(3) Å, *c* = 35.646(3) Å, and *Z* = 4 at 150 K. When A = NH_4^+, M = Fe, Co, Al, the compounds are also orthorhombic (*Pbcn*), with *a* = 10.370(5) Å, 10.340(1) Å, 10.318(7) Å; *b* = 19.588(12) Å, 19.502(1) Å, 19.460(4) Å, *c* = 35.646(3) Å, 36.768(1) Å, 35.808(8) Å at 150 K, respectively, with *Z* = 4. All of the *Pbcn* phases are semiconducting with activation energies between 0.15 and 0.22 eV. For those compounds which are though to contain H_3O^+, Raman spectroscopy or C=C and C–S bond lengths of the BEDT-TTF molecules confirm the presence of H_3O^+ rather than H_2O. In the monoclinic compounds the BEDT-TTF molecules adopt a β" packing motif while in the orthorhombic phases (BEDT-TTF)$_2$ dimers are surrounded by monomers. Raman spectra and bond length analysis for the latter confirm that each molecule of the dimer has a charge of +1 while the remaining donors are neutral. All of the compounds contain approximately hexagonal honeycomb layers of [AM-$(C_2O_4)_3$] and PhCN, with the solvent occupying a cavity bounded by $[M(C_2O_4)_3]^{3-}$ and A. In the monoclinic series each layer contains one enatiomeric conformation of the chiral $[M(C_2O_4)_3]^{3-}$ anions with alternate layers having opposite chirality, whereas in the orthorhombic series the enantiomers form chains whicin each layer. Analysis of the supramolecular organization at the interface between the cation and anion layers shows that this difference is responsible for the two different BEDT-TTF packing motifs, as a consequence of weak H-bonding interactions between the terminal ethylene groups in the donor and the $[M(C_2O_4)_3]^{3-}$ oxygen atoms.

IV-B Solid State Properties of Organic Conductors with π-d Interaction

Some phthalocyanine molecules contain unpaired d-electrons in the conjugated π-electron system. Due to this nature, the itinerant π-electrons coexist with localized unpaired d-electrons in solid phthalocyanine salts, in which a one-dimensional double-chain system (metal and ligand chain) is formed. Furthermore these chains make up wide (π-band) and narrow (d-band) one-dimensional bands. The energy of the narrow band is close to the Fermi energy of the wide band. The phthalocyanine conductor is thus a two-chain and two-band system. The electronic structure of phthalocyanine conductors is analogous to that of the f-electron system, in which a narrow f-band coexists with a wide s-band and they are hybridized near the Fermi level. To understand the electronic structure of this two-band system, we are investigating the charge-transfer salts of NiPc and CoPc and their mixed crystals.

IV-B-1 Preparation and Characterization of Phthalocyanine-Based Organic Alloy $Co_xNi_{1-x}Pc(AsF_6)_{0.5}$ ($0 \leq x \leq 1$)

DING, Yuqin[1]; SIMONYAN, Mkhitar[2]; YONEHARA, Yukako[1]; URUICHI, Mikio; YAKUSHI, Kyuya
([1]GUAS; [2]IMS and Inst. Phys. Res. ARAS)

[*J. Mater. Chem.* **11**, 1469 (2001)]

The organic alloy $Co_xNi_{1-x}Pc(AsF_6)_{0.5}$ ($0 \leq x \leq 1$) was prepared and characterized by elementary analysis (EPMA), X-ray diffraction, ESR, magnetic susceptibility, Raman spectroscopy and reflection spectroscopy. These experiments show that mixed crystals are formed for a wide range of x although $CoPc(AsF_6)_{0.5}$ is not exactly isomorphous to $NiPc(AsF_6)_{0.5}$. The mixing on a molecular level is proved by the x dependence of the ESR and Raman spectra over the whole range of x. The localized spin on Co^{2+} occupies the $3d_{z^2}$ orbital, which is extended to the stacking axis. The reflection spectrum shows that this d orbital forms a one-dimensional band along the stacking axis and closely located near the Fermi level of 3/4-filled π band. We found a very weak $3d_{z^2}$-to-$3d_{x^2-y^2}$ inter-molecular charge transfer transition through the resonance effect of Raman spectrum in the alloy system. Based on the above results, we proposed a model for the energy band near the Fermi level including the 3d bands. This band model explained the differences in the magnetic and optical properties between $CoPc(AsF_6)_{0.5}$ and $NiPc(AsF_6)_{0.5}$.

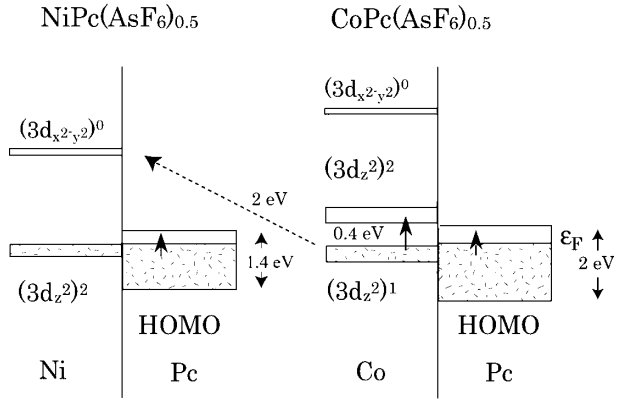

Figure 1. Schematic band structure including 3d bands. The arrows denote the optical transition along the conducting axis detected in the reflection spectra and through resonance effect of Raman spectrum.

IV-B-2 Electronic States and Infrared Spectroscopy of Nickel and Cobalt Phthalocyanines: *Ab initio* Calculations for the Neutral and Cation States

TOMAN, Petr[1]; NESPUREK, Stanislav[1]; YAKUSHI, Kyuya
([1]Inst. Macromolecular Chem. ASCR)

[*Synth. Met.* submitted]

Organic conductors such as TMTSF, BEDT-TTF, and DCNQI have charge sensitive vibrational bands, which show red shift upon oxidation or reduction. This phenomenon comes from the reorganization of the molecular geometry. By contrast, metallophthalocyanine (MPc) has no such vibrational bands, because the molecular geometry is rigid against the oxidation. However, MPc has characteristic vibrational bands, the intensity of which changes upon oxidation. The reason for this change is associated with the change of the charge distribution between neutral and oxidized MPc. We calculated the frequency and intensity of the normal mode of NiPc and CoPc by the B3LYP method. This *ab initio* calculation clearly showed the ligand oxidation both in NiPc and CoPc, which agreed with the experimental observation. Besides, the calculation reproduced the frequency of the infrared-active modes, and the intensity changes of the characteristic bands: the 1291, 1356, 1471, and 1533 cm^{-1} bands of NiPc and 1290, 1468, and 1525 cm^{-1} bands of CoPc.

Using the molecular orbitals, the overlap integrals are calculated between a_{1u} HOMO a MPc and the a_{1g} $3d_{z^2}$ orbital of the adjacent molecule in $MPc(AsF_6)_{0.5}$. The extremely small overlap integral indicates no hybridization between the HOMO band and $3d_{z^2}$ band, in other words, these two bands are almost independent.

IV-B-3 Metal to Insulator Transition of One-Dimensional Bis(1,2-benzoquinonedioximato)-platinum(II), $Pt(bqd)_2$, at Low Temperatures and High Pressures

TAKEDA, Keiki[1]; SHIROTANI, Ichimin[1]; SEKINE, Chihiro[1]; YAKUSHI, Kyuya
([1]Muroran Inst. Tech.)

[*J. Phys: Condens. Matter* **12**, L483 (2000)]

The electrical resistivity of the high quality single crystals of one-dimensional bis(1,2-benzoquinonedioximato)platinum(II), $Pt(bqd)_2$, has been studied at low temperatures and high pressures under hydrostatic conditions. The resistivity along the *c*-axis abruptly decreases with increasing pressure up to 0.9 GPa at room temperature. $Pt(bqd)_2$ with an energy gap of about 0.3 eV at ambient pressure indicates the insulator-to-metal (IM) transition at around 0.8 GPa. The x-ray diffraction and the electronic spectrum of $Pt(bqd)_2$ have been studied at room temperature and high pressures. The mechanism of the IM transition of $Pt(bqd)_2$ is discussed. Below 235 K the resistivity of $Pt(bd)_2$ increases with decreasing temperature at around 0.8 GPa. The metal-to-insulator (MI) transition for $Pt(bqd)_2$ is found at around 235 K under 0.8 GPa. This is the first example that the one-dimensional metal formed from single molecules shows the MI transition at low temperatures.

IV-C Microscopic Investigation of Molecular-Based Conductors

The aim of this research is to clarify the electronic states (charge and spin states) of molecular based compounds with curious electronic phases by microscopic point of view. Although the fundamental properties of molecular based conductors have been very well clarified, it is true that there still remain several unsolved questions in the molecular based conductors.

Microscopic investigations are advantageous for understanding the microscopic charge and spin states. To clarify the low temperature electronic states, we performed the ^{1}H, ^{13}C NMR, and ESR measurements for molecular based conductors.

IV-C-1 Possible Successive SDW Transition in (EDT-TTF)$_2$AuBr$_2$

NAKAMURA, Toshikazu

[*J. Phys. Soc. Jpn.* **69**, 4026 (2000)]

The low temperature magnetic properties in the quasi-one-dimensional system, (EDT-TTF)$_2$AuBr$_2$, were investigated by using ^{1}H-NMR and ESR techniques. (EDT-TTF)$_2$AuBr$_2$ undergoes an SDW transition at 16 K. At 6 K, an anomalous second-peak of ^{1}H-NMR spin-lattice relaxation rate, ^{1}H-T_1^{-1}, in the SDW phase has been observed. An additional increase of ^{1}H-NMR absorption line and gradual decrease of spin-spin relaxation rate, ^{1}H-T_2^{-1}, were observed below 6 K. The magnetic properties of the SDW phase observed in the present salt are discussed from microscopic points of view.

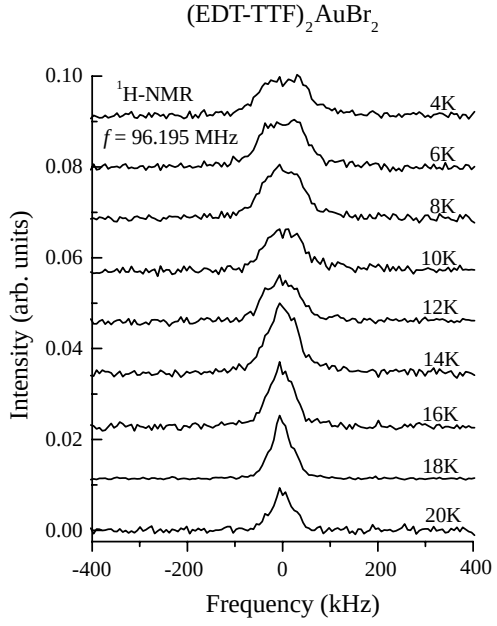

Figure 1. Temperature dependence of the ^{1}H-NMR absorption lines of powdered (EDT-TTF)$_2$AuBr$_2$ crystals.

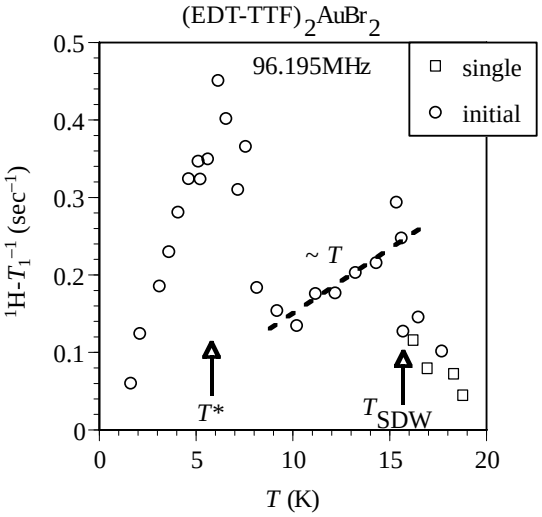

Figure 2. Temperature dependence of the ^{1}H-NMR spin-lattice relaxation rate, T_1^{-1}, in the SDW phase.

IV-C-2 Magnetic Investigation of Organic Conductors Based on TTP Derivatives

TSUKADA, Hiroshi; NAKAMURA, Toshikazu; MISAKI, Yohji[1]; TANAKA, Kazuyoshi[1]
([1]Kyoto Univ.)

[*Synth. Met.* **120**, 869 (2001)]

Magnetic investigation of organic conductors based on TTP derivatives, (BDT-TTP)$_2$SbF$_6$ and (EO-TTP)$_2$AsF$_6$, was carried out by ^{1}H-NMR measurements. The NMR spin-lattice relaxation rates, ^{1}H-T_1^{-1}, of the present salts deviate from the Korringa-like behavior at low temperatures. The low-temperature electronic states of the TTP family will be discussed from microscopic points of view.

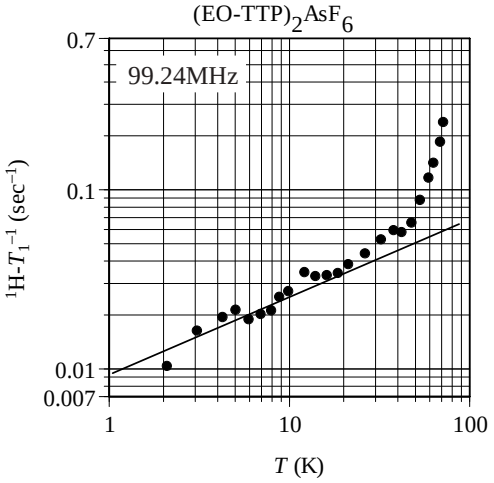

Figure 1. Temperature dependence of the ^{1}H-T_1^{-1} of (EO-TTP)$_2$AsF$_6$.

IV-C-3 Magnetic Properties of Organic Spin-Ladder Systems, (BDTFP)$_2X$(PhCl)$_{0.5}$

NAKAMURA, Toshikazu; TAKAHASHI, Kazuko[1]; ISE, Toshihiro[1]; SHIRAHATA, Takashi[1]; URUICHI, Mikio; YAKUSHI, Kyuya; MORI, Takehiko[2]
([1]Tohoku Univ.; [2]Tokyo Inst. Tech.)

[*Mol. Cryst. Liq. Cryst.* in press]

(BDTFP)$_2X$(PhCl)$_{0.5}$ (X = AsF$_6$, PF$_6$) are quasi-one-dimensional organic conductors with so-called two leg ladder structures; the inter-ladder interaction is one-order smaller than that in intra-ladder. Since there is a considerable dimerization within the column, the upper band is a half-filled.

Figure 1 shows the temperature dependence of the spin susceptibility of the PF$_6$ salt. Between 170 and 300 K, the spin susceptibility is almost temperature independent, but gradually increases as temperature decreases. The EPR signal intensity suddenly decreases below 170 K where the resistivity shows an abrupt jump. The EPR linewidth also shows anomaly; it abruptly decreases around 170 K, suggesting an abrupt change of the relaxation mechanism of the electron spins. It is proved that the low temperature phase of the PF$_6$ salt is spin-singlet.

Figure 2 shows the temperature dependence of the spin susceptibility of the AsF$_6$ salt. In the case of the cooling process, the spin susceptibility abruptly increases around 230 K, suggesting the existence of a phase transition. Below 200 K, the spin susceptibility of the AsF$_6$ salt shows a Curie-like enhancement. This hysteresis phenomenon indicates that the transition is of first order. The low temperature phases are undoubtedly different between the AsF$_6$ and PF$_6$ salts. Below 50 K, the spin susceptibility of the AsF$_6$ salt turns to decrease, indicating spin-gap behavior. It fits with Troyer's prediction for the undoped two-leg ladder. However an abrupt broadening of the EPR line indicates existence of a magnetic order at 14 K.

Although the electronic states of the PF$_6$ and AsF$_6$ salts at R. T. are very similar, those at low temperatures are quite different. Detailed investigations are now going on.

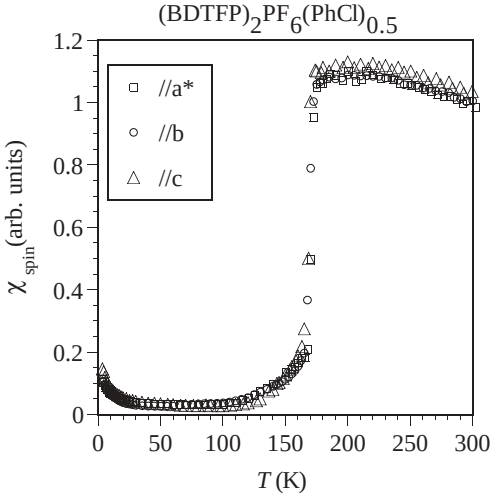

Figure 1. Temperature dependence of the spin susceptibility of (BDTFP)$_2$PF$_6$(PhCl)$_{0.5}$ determined by the EPR signal intensity of a single crystal.

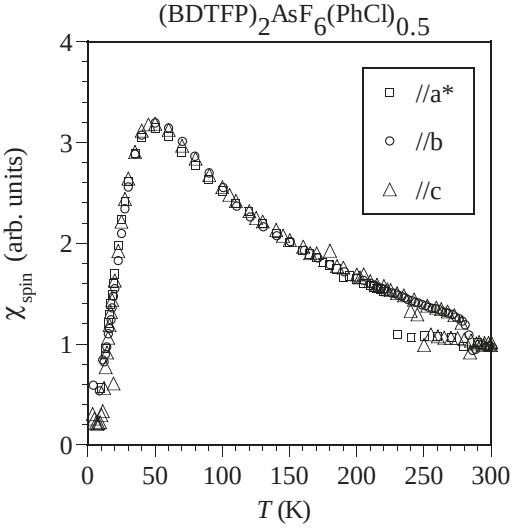

Figure 2. Temperature dependence of the spin susceptibility of (BDTFP)$_2$AsF$_6$(PhCl)$_{0.5}$ determined by the EPR signal intensity of a single crystal.

IV-C-4 EPR Investigation of the Electronic States in β'-type [Pd(dmit)$_2$]$_2$ Compounds (Where dmit is the 1,3-dithia-2-thione-4,5-dithiolato)

NAKAMURA, Toshikazu; TAKAHASHI, Toshihiro[1]; AONUMA, Shuji[2]; KATO, Reizo[2,3]
([1]Gakushuin Univ.; [2]Univ. Tokyo; [3]Inst. Phys. Chem. Res.)

[*J. Mater. Chem.* in press]

Magnetic investigations of organic conductors, β'-type [Pd(dmit)$_2$]$_2$, have been performed by Electron Paramagnetic Resonance (EPR) measurements. We found that most of them except one compound underwent antiferromagnetic transitions. Although they are isostructural with little differences in lattice

parameters, their spin-spin correlations and antiferromagnetic transition temperatures show strong counter ion dependence. The EPR *g*-values of $Pd(dmit)_2$ cannot be explained within the framework of isolated radical description, which is a good approximation for conventional organic conductors. The electronic structures of a series of molecular conductors based on $Pd(dmit)_2$ at ambient pressure are discussed from microscopic points of view.

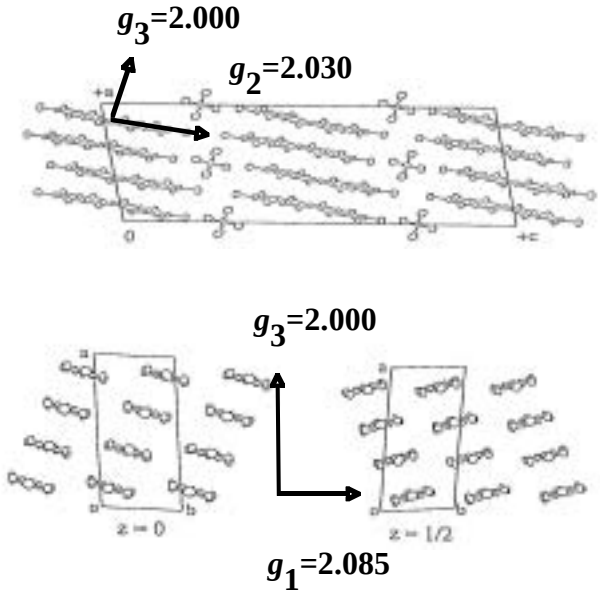

Figure 1. Determined principal axes and values β'-Et_2Me_2P-$[Pd(dmit)_2]_2$ on the actual crystal structure.

IV-C-5 Microscopic Investigation of Itinerant and Local Spins System, $(CHTM\text{-}TTP)_2TCNQ$

NAKAMURA, Toshikazu; TANIGUCHI, Masateru[1]; MISAKI, Yohji[1]; TANAKA, Kazuyoshi[1]; NOGAMI, Yoshio[2]
([1]Kyoto Univ.; [2]Okayama Univ.)

$(CHTM\text{-}TTP)_2TCNQ$ is a new organic conductor developed by Kyoto university group. This compound is composed of segregated donor (CHTM-TTP) and acceptor (TCNQ) layers. The CHTM-TTP molecules stack to form one-dimensional columns. On the other hand, there is little interaction between the TCNQ molecules. This salt shows metallic behavior down to 30 K with abrupt jump around 240 K. In order to clarify the low temperature electronic phases of this salt, we performed magnetic investigation.

Figure 1 shows the temperature dependence of the spin susceptibility determined by the EPR signal intensity. Between 240 K and 300 K, the spin susceptibility shows a gradual increase as the temperature decreases. At 240 K and 170 K, the spin susceptibility decreases abruptly. The principal values of the *g*-tensor change their absolute values both at the transition temperatures. It cannot be explained within the framework of one spin picture . These observations lead us to a conclusion that effective local moments on TCNQ decrease at 240 K, and that disappear perfectly below 170 K.

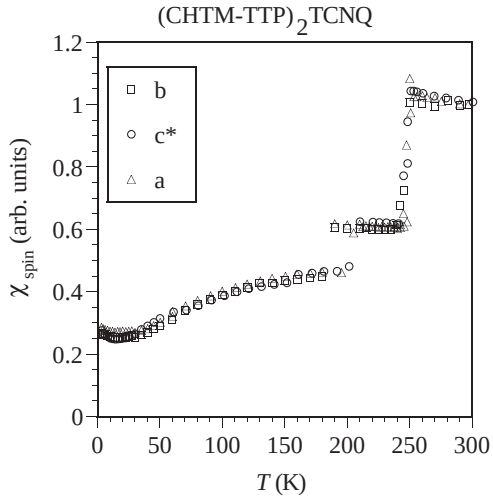

Figure 1. Temperature dependence of the spin susceptibility of $(CHTM\text{-}TTP)_2TCNQ$ determined by the EPR signal intensity of a single crystal.

IV-D Development of Magnetic Organic Superconductors and Related Systems

Although the first organic superconductor $(TMTSF)_2PF_6$ called Bechgaard salt possesses one-dimensional electronic band structure, its crystal structure gave a large hint to design two-dimensional metals without one-dimensional metal instabilities. In fact, with the aid of the guiding principle on the design of molecular conductors based on simple extended Hückel tight binding band picture, we could find the first κ-type organic superconductor with typical two-dimensional cylindrical Fermi surface in 1987 (κ-ET_2I_3). Since a number of κ-type organic superconductors including the system with the highest-T_c record (κ-$ET_2Cu[N(CN)_2]Cl$; T_c = 12.8 K at 0.3 kbar) have been discovered and the κ-type molecular conductors are nowadays regarded as the most typical two-dimensional metals. However the recent development of the simple typical organic superconducting systems becomes somewhat stagnant in the last decade. On the other hand, an increasing interest is going to be attracted to the magnetic organic conducting systems where the magnetic order and superconductivity are expected to coexist.

We have recently found the systems exhibiting unprecedented superconductor-to insulator transition and the first antiferromagnetic organic superconductor constructed of BETS (= bis(ethylenedithio)tetraselenafulvalene) molecules and magnetic anions containing Fe^{3+}. Furthermore, we have recently discovered a field-induced superconducting transition in another type of two-dimensional conductor, λ-$BETS_2FeCl_4$.

IV-D-1 Magnetic-Field Induced Superconductivity in a Two-Dimensional Organic Conductor

UJI, Shinya[1]; SHINAGAWA, Hideyuki[1]; TERASHIMA, Taichi[1]; YAKABE, Taro[1]; TERAI, Yoshikazu[1]; TOKUMOTO, Madoka[2]; KOBAYASHI, Akiko[3]; TANAKA, Hisashi; KOBAYASHI, Hayao

([1]Natl. Res. Inst. Metal; [2]Electrotechnical Lab.; [3]Univ. Tokyo)

[*Nature* **410**, 908 (2001)]

The application of sufficiently strong magnetic field to superconductor will, in general, destroy the superconducting state. Two mechanisms are responsible for this. The first is the Zeeman effect, which breaks apart the paired electrons if they are in a spin-singlet (but not a spin-triplet) state. The second is the so-called orbital effect, whereby the vortices penetrate into the superconductors and the energy gain due to the formation of the paired electrons is lost. In this paper we have reported resistance and magnetic torque experiments on single crystals of the quasi-two-dimensional organic conductor λ-$(BETS)_2FeCl_4$, where the field-induced insulator-to metal transition has been previously discovered around 10 T. We found that for magnetic fields applied exactly parallel to the conducting layers of the crystals, superconductivity is induced for fields above 17 T at a temperature of 0.1 K. The resulting phase diagram indicates that the transition temperature increases with magnetic field.

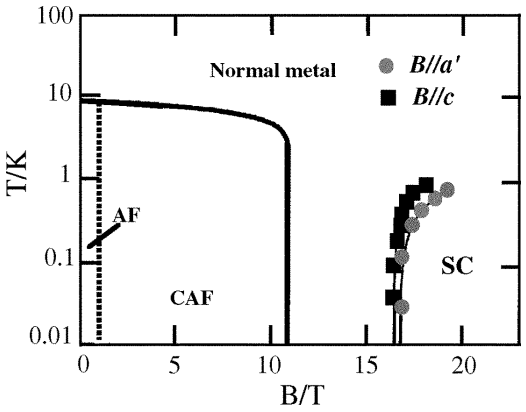

Figure 1. Temperature versus magnetic field diagram for λ-$(BETS)_2FeCl_4$.

IV-D-2 Superconductivity in an Organic Insulator at Very High Magnetic Fields

BALICAS, Luis[1]; BROOKS, James[1]; STORR, Kevin[1]; UJI, Shinya[2]; TOKUMOTO, Madoka[3]; TANAKA, Hisashi; KOBAYASHI, Hayao; KOBAYASHI, Akiko[4]; BARZYKIN, Victor[1]; GOR'KOV, Lev[1]

([1]Florida State Univ.; [2]Natl. Res. Inst. Metal; [3]Electrotechnical Lab.; [4]Univ. Tokyo)

[*Phys. Rev. Lett.* **87**, 067002-1 (2001).]

We investigated by electrical transport the field-induced superconducting state (FISC) in the organic conductor λ-$BETS_2FeCl_4$. Below 4 K, antiferromagnetic-insulator, metallic and eventually superconducting (FISC) ground state are observed with increasing in-plane magnetic field. As shown in Figure 1, the superconducting state develops progressively with decreasing temperature but is suppressed for fields sufficiently away from 33 T. The temperature-magnetic field phase diagram shows the maximum temperature of the FISC phase of about 4.2 K is realized around 33 T, which is lower than T_c of λ-$BETS_2GaCl_4$ (≈ 5.5 K). The

FISC state survives between 18 and 41 T and can be interpreted in terms of the Jaccarino-Peter effect, where the external magnetic field compensates the exchange field of aligned Fe^{3+} ions. We further argue that the Fe^{3+} moments are essential to stabilize the resulting singlet, two-dimensional superconducting state.

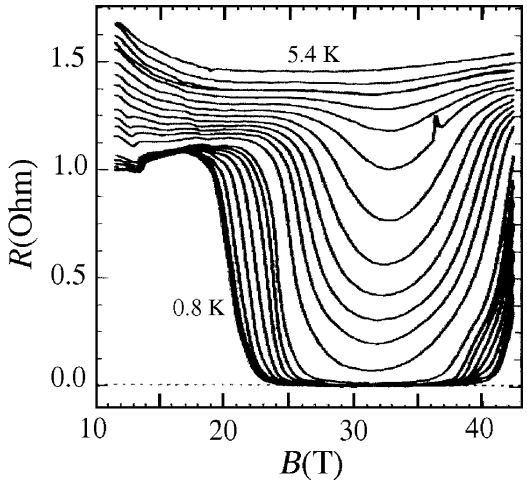

Figure 1. Resistance as a function of magnetic field *B*, applied along the in-plane *c* axis of λ-$BETS_2FeCl_4$ single crystal for temperature intervals of approximately 0.25 K, between 5.4 and 0.8 K.

IV-D-3 Novel Electronic Property in Organic Conductor: Superconductivity Stabilized by High Magnetic Field

UJI, Shinya[1]; KOBAYASHI, Hayao; BROOKS, James[2]
([1]Natl. Res. Inst. Metal; [2]Florida State Univ.)

[*Adv. Mater.* in press]

Organic conductors have attracted considerable interest because of the characteristic properties relating to their low dimensionality of the electronic states. Among various organic conductors, λ-$(BETS)_2FeCl_4$ is one of the most attractive materials in the last decade because strong competition is expected between the antiferromagnetic order of the Fe moments and the superconductivity. λ-$(BETS)_2FeCl_4$ is known to have a unique phase diagram. At zero magnetic field, it shows a metal-insulator transition around 8 K, while the isostructural non-magnetic salt λ-$(BETS)_2GaCl_4$ undergoes a superconducting transition around 6 K. The metal-insulator transition in λ-$(BETS)_2FeCl_4$ is associated with the antiferromagnetic (AF) order of the Fe moments with the spins $S = 5/2$. The insulating phase is destabilized by the magnetic field above about 10 T, and a paramagnetic metallic state with ferromagnetically oriented Fe^{3+} spins is recovered. Furthermore, a field-induced superconductivity (FISC) has been recently discovered at 18–41 T. FISC has been reported for a Chevrel compounds $Eu_xSn_{1-x}Mo_6S_8$ with $T_c = 3.8$ K. As field increases, the superconductivity is destroyed at about 1 T but is restored by the field of 4 T below 0.1 K. This phenomenon is understood in terms of Jaccarino-Peter (J-P) compensation effect. Due to the antiferromagnetic coupling between the Eu spins and the conduction electrons, the exchange polarization can be compensated by an external field leading to the reappearance of superconductivity (FISC) at high magnetic field. J-P effect is considered to be essential also for FISC of λ-$(BETS)_2FeCl_4$.

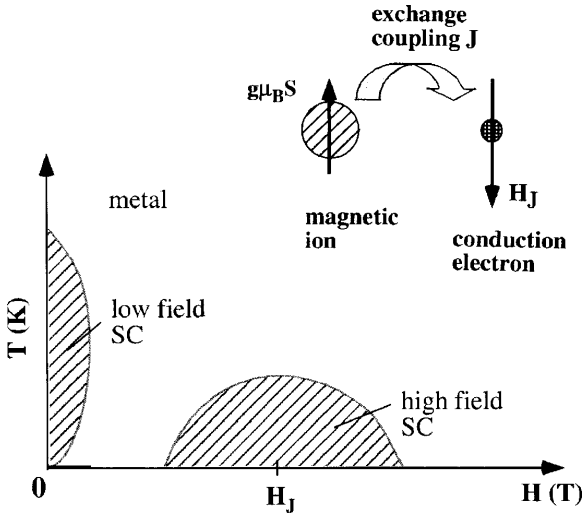

Figure 1. Schematic phase diagram of the system showing FISC and schematic picture of J-P effect.

IV-D-4 Field-Induced Superconducting Phase of λ-$(BETS)_2Fe_xGa_{1-x}Cl_4$

KOBAYASHI, Hayao; TANAKA, Hisashi; ZHANG, Bin; KOBAYASHI, Akiko[1]; TOKUMOTO, Madoka[2]; UJI, Shinya[3]; BROOKS, James[4]
([1]Univ. Tokyo; [2]Electrotechnical Lab; [3]Natl. Res. Inst. Metal; [4]Florida State Univ.)

About a decades ago, we have tried to develop a series of BETS conductors with magnetic anions, with the aim of studying the π-d interaction in organic conductors. In fact, many interesting phenomena have been found in λ- and κ-$(BETS)_2FeX_4$ (X = Cl, Br). For example, λ-$(BETS)_2FeCl_4$ exhibits various phase transitions: (1) At ambient pressure, the system undergoes a coupled antiferromagnetic (AF) and insulating transition around 8.5 K. (2) At high pressure, this AF insulating state is suppressed and the superconducting phase is stabilized (> 3 kbar). (3) Furthermore, by applying magnetic field, the ground state is changed as, the AF insulating state → metallic state → superconducting state → metallic state with increasing magnetic field. In addition, with decreasing temperature, the alloy system, λ-$(BETS)_2Fe_xGa_{1-x}FeCl_4$ ($0.35 < x < 0.5$) exhibits the transitions as, metallic state → insulating state → superconducting state. We have recently examined the resistivities of λ-$(BETS)_2Fe_xGa_{1-x}FeCl_4$ ($x \approx 0.35$), which exhibits a subsequent metal → superconductor → insulator transition at zero magnetic field. The superconducting state can survive up to 15 T (= maximum field in this study) when magnetic field is approximately parallel to the conduction plane. Considering that the superconducting state of λ-$(BETS)_2GaCl_4$ is broken above 10 T, the phase diagram shown in Figure 1 is of special interest.

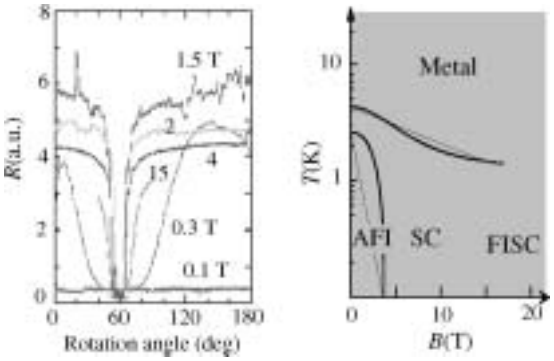

Figure 1. (a) Resistivity of λ-$(BETS)_2Fe_xGa_{1-x}FeCl_4$ ($x \approx 0.35$) for various orientation of the crystal ($T \approx 1$–3 K) (b) Schematic *T*-*B* phase diagram.

IV-D-5 Antiferromagnetic Ordering of Fe^{3+} Ions in Organic Superconductor, κ-$BETS_2FeCl_xBr_{4-x}$

FUJIWARA, Emiko; FUJIWARA, Hideki; KOBAYASHI, Hayao; KOBAYASHI, Akiko[1]
([1]Univ. Tokyo)

Recently we have found the first and second antiferromagnetic organic superconductors, κ-$BETS_2FeX_4$ (X = Br and Cl) which undergo antiferromagnetic transitions at 2.5 K (Br) and 0.6 K (Cl) and a superconducting transitions at 1.1 K (Br) and 0.1 K (Cl). In this work, the magnetic and electrical properties of κ-$BETS_2FeCl_xBr_{4-x}$ were examined by using one single crystal. The temperature dependence of the magnetic susceptibility and the field (*H*) dependence of the magnetization (*M*) at 2 K of κ-$(BETS)_2FeCl_xBr_{4-x}$ revealed that the Néel temperature (T_N) shifts to lower temperature with the increase of chlorine contents (*x*). Moreover, the easy spin axis was found to rotate from the direction parallel to *a* axis to *b* axis with increasing *x*. In other words, though the metamagnetic behavior of pure $FeBr_4$ system ($x = 0$) was observed for the magnetic field parallel to *a*, that of the $FeClBr_3$ system ($x = 1.0$) was observed for the field parallel to *b*. The magnetic field dependence of the electrical resistivities showed that both T_N where the resistivity step was observed and T_c decreased rapidly with the increase of *x*.

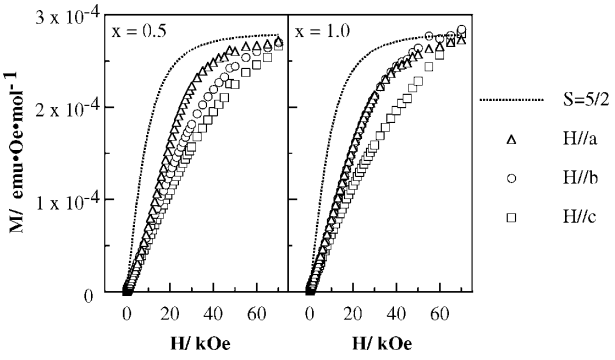

Figure 1. (a) Field (*H*) dependence of the magnetization (*M*) at 2.0 K of κ-$(BETS)_2FeCl_xBr_{4-x}$ ($x \approx 0.5$ and 1.0). The field were applied along the three axes of crystal lattices. The Brillouin function with $S = 5/2$ is also shown for comparison.

IV-D-6 The *x*-Dependence of Electrical Properties and Antiferromagnetic Ordering between Fe^{3+} Ions in κ-$BETS_2Fe_{1-x}Ga_xBr_4$ System

FUJIWARA, Hideki; FUJIWARA, Emiko; KOBAYASHI, Hayao; KOBAYASHI, Akiko[1]
([1]Univ. Tokyo)

As reported before, both κ-$BETS_2FeBr_4$ and κ-$BETS_2GaBr_4$ salts are isostructural to each other and showed superconductivity around 1 K, but the transition of $GaBr_4^-$ salt is very broad compared to the case of $FeBr_4^-$ salt. Furthermore, $FeBr_4^-$ salt exhibited the antiferromagnetic ordering of Fe^{3+} spins at 2.5 K. Therefore we have measured the magnetic and electrical properties of the alloy system κ-$BETS_2Fe_{1-x}Ga_xBr_4$ to investigated the gallium contents-dependence of the antiferromagnetic ordering of Fe^{3+} spins and the superconducting state. The temperature dependence of the magnetic susceptibility of κ-$BETS_2Fe_{1-x}Ga_xBr_4$ (Ga = 0.1 and 0.2) revealed that the Néel temperature shifts to lower temperature with the increase of the gallium contents (2.3 K for $x = 0.1$ and 2.1 K for $x = 0.2$). On the other hand, the measurement of the electrical resistivities of κ-$BETS_2Fe_{0.9}Ga_{0.1}Br_4$ showed that the temperature of the step-like drop of resistivities, which is in good agreement with the Néel temperature determined from the magnetic measurement, also shifts to lower temperature (2.3 K) with the increase of the gallium contents. On the other hand, the mid-point of the critical temperature of superconductivity is almost the same as that of the κ-$BETS_2FeBr_4$ salt (1.1 K), but the transition became broader than the case of the κ-$BETS_2FeBr_4$ salt.

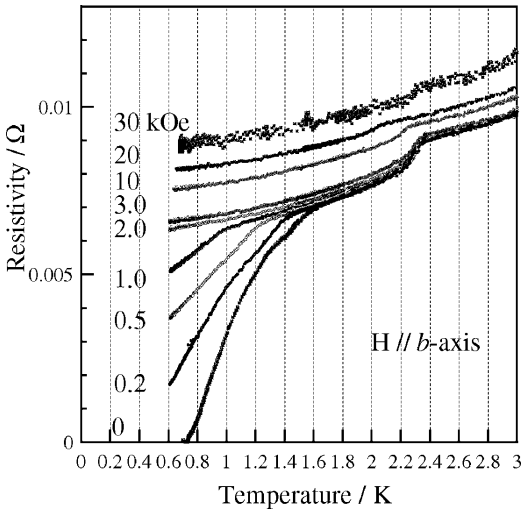

Figure 1. Magnetic field dependence of the electrical resistivities of κ-$BETS_2Fe_{0.9}Ga_{0.1}Br_4$.

IV-D-7 Organic Antiferromagnetic Metals Exhibiting Superconducting Transitions κ-$(BETS)_2FeX_4$ (X = Cl, Br): Drastic Effect of Halogen Substitution on the Successive Phase Transitions

OTSUKA, Takeo[1]; KOBAYASHI, Akiko[1];

MIYAMOTO, Yasuhisa[1]; WADA, Nobuo[1]; FUJIWARA, Emiko; FUJIWARA, Hideki; KOBAYASHI, Hayao
([1]Univ. Tokyo)

[*J. Solid State Chem.* **159**, 407 (2001)]

The magnetic and thermal properties of an organic conductor incorporating localized magnetic moments, κ-$(BETS)_2FeCl_4$ were investigated down to 60–70 mK. Similar to the Br analogue κ-$(BETS)_2FeBr_4$, κ-$(BETS)_2FeCl_4$ exhibited a successive antiferromagnetic and superconducting transitions with lowering temperature (T_N = 0.45 K, T_c = 0.1 K). That is, κ-$(BETS)_2FeCl_4$ is the second antiferromagnetic organic metal which exhibits a superconducting transition at ambient pressure. It became clear that the halogen exchange (Br → Cl) in the anions results in the strong reduction of both magnetic and superconducting transition temperatures. Resistivities showed a small drop at 0.45 K (= T_N), which gave a direct evidence of the existence of π-d interaction between π metal electrons and localized magnetic moments of Fe. In contrast to κ-$(BETS)_2FeBr_4$ exhibiting three-dimensional nature of the magnetic transition, the specific heat of κ-$(BETS)_2FeCl_4$ indicates the low-dimensionality of the spin system.

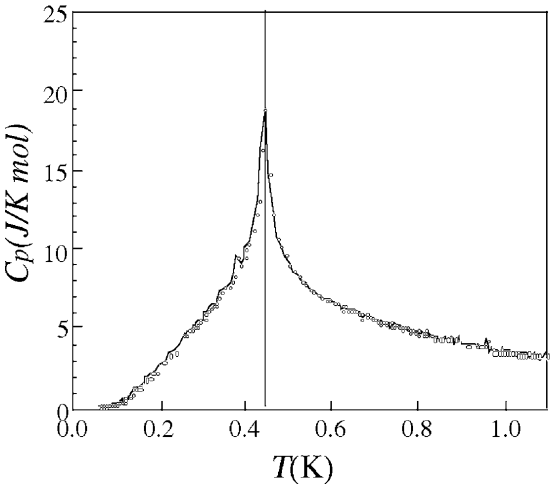

Figure 1. The specific heat of κ-$(BETS)_2FeCl_4$.

IV-D-8 A New Molecular Superconductor, κ-$(BETS)_2TlCl_4$

GRITSENKO, Victor; TANAKA, Hisashi; KOBAYASHI, Hayao; KOBAYASHI, Akiko[1]
([1]Univ. Tokyo,)

[*J. Mater. Chem.* in press]

Since the first discovery of the κ-type organic superconductor, κ-ET_2I_3 in 1987, many organic superconductors with κ-type molecular packing were discovered. Among them, κ-$ET_2Cu[N(CN)_2]Cl$ reported in 1990 has retained the highest Tc-record of organic superconductor (T_c = 12.8 K) for more than 10 years. About a decade ago, we have examined seven BETS conductors with tetrahalide anions MX_4 (M = Fe, Ga, In; X = Cl, Br) from which five organic superconductors including the first antiferromagnetic organic superconductor, κ-$(BETS)_2FeBr_4$ have been discovered so far. Recently we have examined the electrical resistivity of κ-$(BETS)_2TlCl_4$. Contrary to our previous experiments showing that the crystal was broken around 220 K, we found that the crystal could survive down to low temperatures when the cooling speed was very large. This accidental finding suggests that the resistivity measurements of this system can be made down to low temperature if the destruction of the crystal around 220 K is suppressed. Accordingly we tried to perform the resistivity measurements by using the crystal coated by epoxy resin under the expectation that "effective pressure" produced by the contraction of the epoxy resin at low temperatures will suppress the destruction of the crystal around 220 K. As was expected, we could observed the superconducting transition despite of the remaining large resistivity anomaly around 220 K.

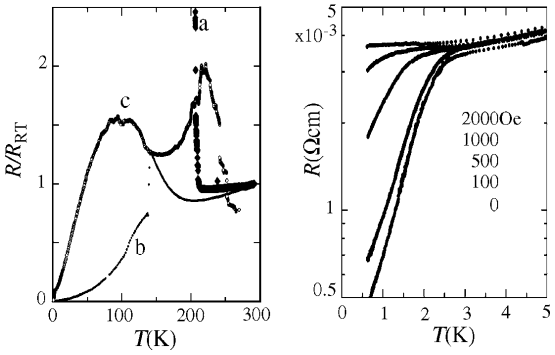

Figure 1. (a) Temperature dependence of resistivity of κ-$(BETS)_2TlCl_4$. a: slow cooling, b: fast cooling, c: slow cooling with epoxy resin. (b) Superconducting transition.

IV-D-9 Structure and Physical Properties of Divalent Magnetic Anion Salts Based on BETS Molecule

FUJIWARA, Emiko; GRITSENKO, Victor; FUJIWARA, Hideki; TAMURA, Itaru; KOBAYASHI, Hayao; TOKUMOTO, Madoka[1]; KOBAYASHI, Akiko[2]
([1]IMS and Electrotec. Lab.; [2]Univ. Tokyo)

With the aim of the development of new magnetic conductors, we have investigated BETS salts involving divalent transition metal halides such as the $CoCl_4^{2-}$, $CoBr_4^{2-}$ and $MnBr_4^{2-}$ anions with magnetic moments. X-Ray crystal structure analysis of the $CoCl_4^{2-}$ salt cleared that the salt is the κ-$(BETS)_4CoCl_4(EtOH)$. κ-$(BETS)_4CoCl_4(EtOH)$ showed metallic conducting behavior down to 0.7 K and its room temperature conductivity is 1–10 $S\cdot cm^{-1}$, which is consistent with the result of band structure calculation giving conventional two-dimensional Fermi surfaces. Crystal structure analysis of the $MnBr_4^{2-}$ salt indicated that the salt is θ-$(BETS)_4MnBr_4(EtOH)_2$. (Figure 1) The electrical and magnetic properties of θ-$(BETS)_4MnBr_4(EtOH)_2$ showed that the system is metallic down to *ca.* 30 K with room temperature conductivities of 10–100 $S\cdot cm^{-1}$ and there is only a slight antiferromagnetic interaction between the manganese 3d spins because of

anion-solvent-intermingled layer structure. With regard to the $CoBr_4^{2-}$ salt, the conducting behavior is almost the same as that of the $MnBr_4^{2-}$ salt.

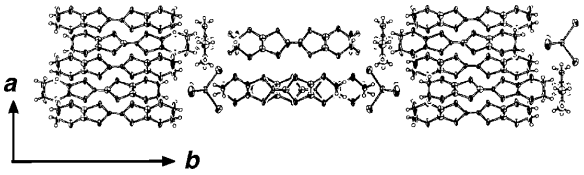

Figure 1. Crystal structure of θ-$(BETS)_4MnBr_4(EtOH)_2$ projected on to the *ac*-plane.

IV-D-10 Novel Molecular Metals Exhibiting Peculiar Magnetism Originating From Lanthanide *f* Electrons

OTSUKA, Takeo[1]; CUI, Hengbo[1]; KOBAYASHI, Akiko[1]; MISAKI, Yohji[2]; KOBAYASHI, Hayao
([1]Univ. Tokyo; [2]Kyoto Univ.)

Compared with the *d*-block elements, *f*-block elements, lanthanides, will show still more unique electronic properties because of the peculiar magnetic properties of *f* orbital spins, and large magnetic moments. Since the *f* electrons are considered to be shielded by outer electrons, the spin-orbit coupling is believed to play essential role in the magnetic properties. Though the molecular metals incorporating localized *f* electrons are still very rare, the study of the '*f*-π system' will undoubtedly expand the range of functional molecular materials. We have examined the crystal structures, electronic conductivities and magnetic properties of $(BDT\text{-}TTP)_5[M(NO_3)_5]$ (BDT-TTP = 2,5-bis(1,3-dithiol-2-ylidene)-1,3,4,6-tetrathiapentalene; M = Sm, Eu). The 4-probe resistivities measurements of $(BDT\text{-}TTP)_5[M(NO_3)_5]$ (M = Eu, Sm) showed the systems to be metallic down to 2 K, which is consistent with the two-dimensional electronic band structures. The *dc* magnetic susceptibilities were measured on SQUID (Figure 1). At first sight, weakly temperature-dependent paramagnetic susceptibility at high temperature region seems to suggest Pauli paramagnetism. The susceptibility value, however, exceeds 10^{-3} emu/mol. A contribution from Eu^{3+} ion should be taken into account. The energy levels of the lowest excited state (J = 1) and the ground state (J = 0) is very close for Eu^{3+} ion, and the excited state is easily accessed by thermal excitation. In this case, the Van Vleck paramagnetic compensation term is important. Similar but smaller Van Vleck paramagnetism was also observed in Sm system.

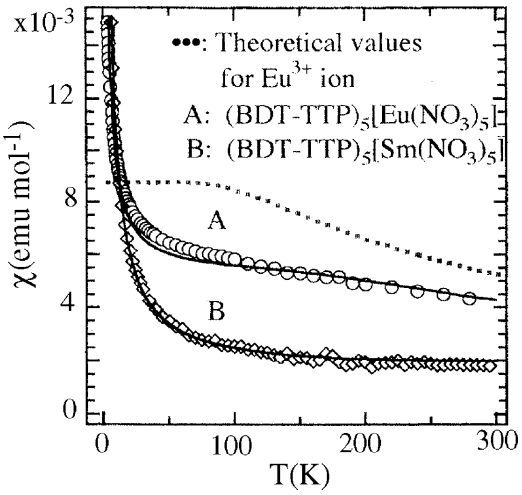

Figure 1. Paramagnetic susceptibility of $(BDT\text{-}TTP)_5[M(NO_3)_5]$ (M = Eu (A), Sm (B)). The dotted curve shows the Van Vleck paramagnetism of Eu^{3+} ion.

IV-E Crystal Structure Analyses at Low Temperature and/or High Pressure

Since the molecular crystal is very soft and rich in the structural freedom, various structural phase transitions are expected by applying pressure and/or lowering temperature. Therefore the precise three-dimensional X-ray structure analyses at high pressure and/or low temperature are very important in the studies of solid state physics and chemistry of molecular crystals. The apparatus used for our present low-temperature crystal structure analyses is essentially the same to the IP (imaging plate) X-ray system equipped with liquid helium refrigerator established by us about 10 years ago. But the accuracy of the structure analysis was enhanced greatly owing to the recent slight remodeling of the apparatus. Concerning to the high-pressure X-ray structural studies, we are trying to establish the X-ray studies by combining diamond anvile cell and the IP system mentioned above. To our knowledge, accurate X-ray crystal structure determination of the soft organic crystal by diamond anvile high-pressure cell is still very rare. Very recently we have performed precise single crystal X-ray structure analysis of the crystal of organic conductor up to 2 GPa. There seems to be no difficulty to elevate the pressure up to about 5 GPa. As for the high-pressure resistivity measurements, we have recently reported the improved method of four-probe resistivity measurements for soft organic single crystals.

IV-E-1 Doubling of Lattice Constants of New Organic Superconductor κ-$(BETS)_2TlCl_4$

TAMURA, Itaru; TANAKA, Hisashi; KOBAYASHI, Hayao; KOBAYASHI, Akiko[1]
([1]Univ. Tokyo)

About a decade ago, we have examined the crystal structure and electronic properties of BETS conductors with tetrahalide anions such as FeX_4^- and GaX_4^- (X = Cl, Br). Among them, three superconductors with κ-type molecular arrangements have been discovered, suggesting the ground state of κ-type BETS conductor with MX_4^- anion to be superconducting. However, from the early days of the studies of κ-$BETS_2MX_4$, it was noticed that the accurate resistivity measurements of κ-type BETS salts with relatively large anions such as $FeBr_4^-$ and $GaBr_4^-$ are difficult because the crystals frequently show small resistivity jumps. Very recently we have discovered the superconductivity of the crystal of κ-$BETS_2TlCl_4$ coated with epoxy resin (fourth κ-type BETS superconductor). But the crystal without epoxy resin was always broken around 200 K, which had prevented further studies of this system. The crystal of κ-$BETS_2TlCl_4$ has orthorhombic unit cell with the space group of Pnma. In order to examine the crystal structure of this new organic superconductor, we have tried to examine X-ray diffraction patterns at low temperature by using the crystal coated by epoxy resin and found the doubling of the lattice constant *c* at low temperature (see Figure 1). The lattice constants were determined as: at room temperature, *a* = 11.626(2) Å, *b* = 36.618(8), *c* = 8.560(6); at 20 K, *a* = 11.434(1) Å, *b* = 36.379(5), *c* = 16.897(5).

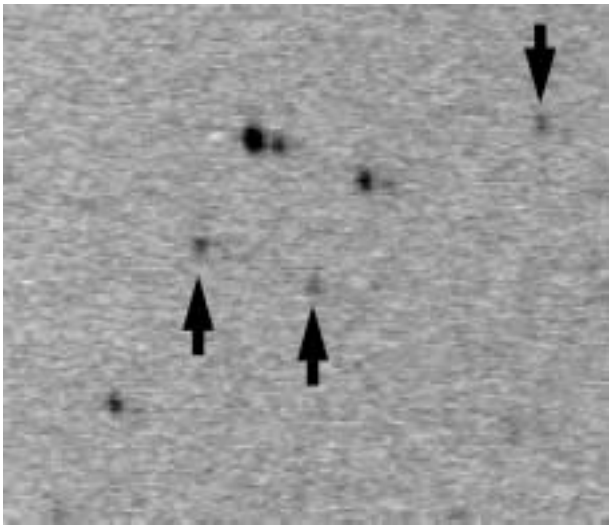

Figure 1. X-ray diffraction pattern of κ-$BETS_2TlCl_4$ at 20 K. The arrows indicate new diffraction spots developed at low temperature.

IV-E-2 High-Pressure Structure of α-(BEDT-TTF)$_2$I$_3$

TAMURA, Itaru; KOBAYASHI, Hayao

α-ET_2I_3 is one of the representative organic conductors, which undergoes a metal-insulator transition at about 135 K at ambient pressure. This metal-insulator transition is suppressed at high pressure and disappears at about 1.5 GPa. Recently, the peculiar transport property of this system observed at high pressure attracts many interests. We performed X-ray structure analyses of α-ET_2I_3 single crystal under several pressures using Diamond-anvil cell. The sample was put in a hole of gasket mounted on the Diamond anvil with 1.0 mm culet-diameter. Single crystals of α-ET_2I_3, with typical dimension of $0.28 \times 0.23 \times 0.15$ mm^3 were used. Pressures were determined by ruby fluorescence method. X-Ray intensity data were collected by using the IP system. The oscillation photographs were taken by using a rotating anode X-ray generator with a Mo target. The lattice parameters were decreased isotropically with increasing pressure. Isotropic thermal parameters were used for all the atoms except three I atoms. The reliability factor was reduced to about 8%. Usually the bond lengths within molecules are believed to be unchanged at low pressure region. However, the I–I bond length was fairly shortened with increasing pressure (Figure 1). The data collections under higher pressures are now underway.

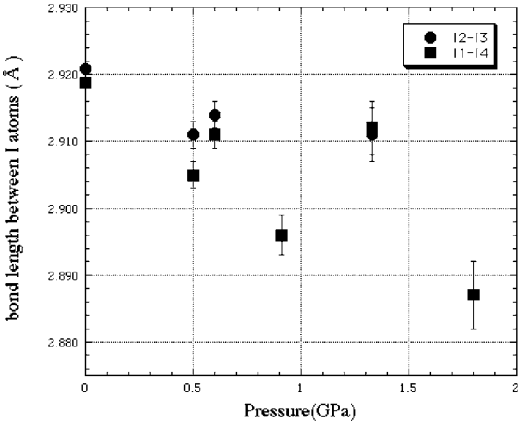

Figure 1. The pressure dependence of I–I bond length.

IV-F Development of New Molecular Conductors

The design and development of new functional molecules are most important for the progress in the field of molecular assemblies. Since the discovery of the first organic superconductors by Bechgaard and Jerome in 1980, an extremely large progress has been made in the field of molecular conductors. It is well known that all the molecular metals ever developed are the systems consisted of more than two components because the charge transfer between the molecules consisting conduction band and other molecules (or ions) has been considered to be indispensable for the carrier generation in organic systems. This means that the molecular crystal consisted of single-component molecules must be non-metallic because of the lack of the charge carriers. However, we have recently developed the first molecular metal composed of single-component molecules. This finding will indicate the possibility of the

development of various unprecedented molecular conductors such as (1) superconductors composed of single-component molecules, (2) ferromagnetic metal composed of single-component magnetic molecules and (3) molecular metals soluble in organic solvents. These systems will be future targets. In addition, we are now trying to develop pure organic ferromagnetic metal based on π donor molecules containing stable radical parts.

IV-F-1 Molecular Design and Development of Single-Component Molecular Metals

KOBAYASHI, Akiko[1]; TANAKA, Hisashi; KOBAYASHI, Hayao
([1]Univ. Tokyo)

[*J. Mater. Chem.* in press]

We have examined the requirements for designing single component molecular metals, based on the results of crystal structure analyses, electrical resistivity measurements and extended Hückel tight-binding band calculations of molecular conductors composed of single-component molecules of $[Ni(ptdt)_2]$ with extended TTF-ligands, ptdt. The design of π molecules with a small HOMO-LUMO gap and a TTF-like skeleton is a key step to developing single-component molecular metals. A new approach is proposed to reduce HOMO-LUMO gaps. A single-component three-dimensional molecular metal based on an analogous neutral transition metal complex molecule, $[Ni(tmdt)_2]$ were prepared and characterized. Black crystals of this compound were obtained by the electrochemical method. In the crystal, which has a triclinic unit cell containing only one molecule, the planar $[Ni(tmdt)_2]$ molecules are closely packed to form the lattice plane (021-). There are intermolecular short S···S contacts which indicate that the system is a three-dimensional conductor. The resistivity measurements shows that the system is metallic down to 0.6 K. The extended Hückel tight-binding band calculation gave three-dimensional semi-metallic Fermi surfaces. A metallic crystal was also prepared with an analogous molecule $[Ni(dmdt)_2]$. The formation of a single component molecular metal opens the possibilities of developing various types of unprecedented functional molecular systems such as single component molecular superconductors, ferromagnetic single-component molecular metals, molecular metals (or superconductors) soluble in organic solvent, *etc.*

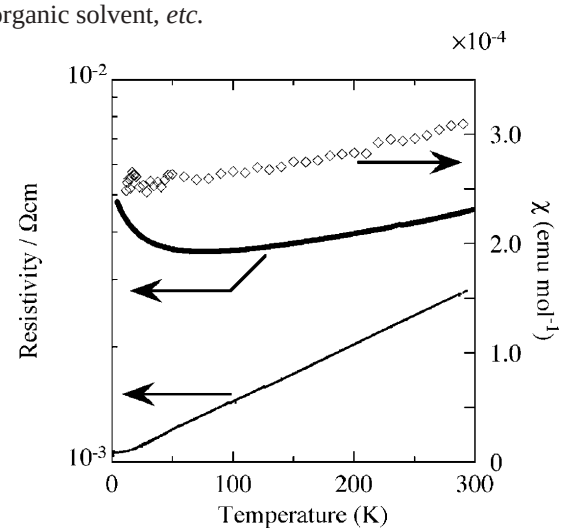

Figure 1. The susceptibility (upper) and resistivities of compacted pellet (middle) and single crystal (lower) of $[Ni(tmdt)_2]$.

IV-F-2 Single Component Conductors Containing Magnetic Transition Metals

TANAKA, Hisashi; KOBAYASHI, Hayao; KOBAYASHI, Akiko[1]
([1]Univ. Tokyo)

We have recently succeeded to develop the first three-dimensional molecular metal composed of single component molecules, $[Ni(tmdt)_2]$, where tmdt (= trimethylenetetrathiafulvalenedithiolate) is a extended-TTF ligand. Since the single component molecular metal has been realized, one of the next targets will be the development of single component magnetic molecular metals. We have prepared metal complexes with magnetic ions (Cu^{2+}, Co^{2+}, *etc.*) coordinated by tmdt and dmdt (dmdt = dimethyltetrathiafulvalene-dithiolate). These complexes were easily oxidized by electrochemical methods. Black crystals of neutral metal complexes were obtained for $[Cu(dmdt)_2]$ and the resistivity measurement was made on a compaction pellet sample. The room temperature conductivity was considerably high as for the compaction sample (3.0 Scm^{-1}) and the activation energy was very small (E_a = 60 meV). The susceptibility was consistent with the existence of localized magnetic moment of Cu^{2+}. Small antiferromagnetic interaction was observed between Cu^{2+} ions (C = 0.327(3) emu K mol^{-1}, Θ = –4.18(6) K). X-Ray crystal structure analysis showed that $[Cu(dmdt)_2]$ is a non-planar molecule though the dmdt ligand moiety is ideally planar. Four sulfur atoms of two bidentate ligands coordinate the central copper atom with a distorted tetrahedral geometry.

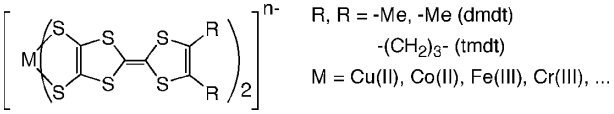

Scheme 1.

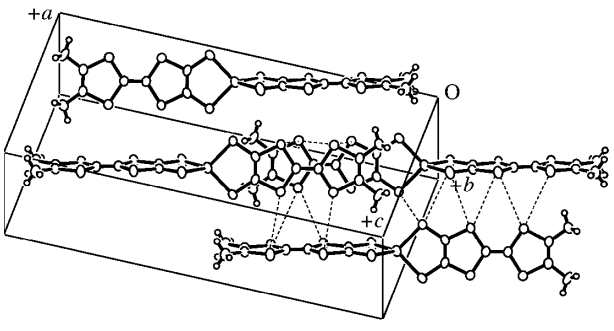

Figure 1. Crystal structure of $[Cu(dmdt)_2]$.

IV-F-3 Synthesis, Structures and Properties of New Organic Donors Connecting to a TEMPO Radical Through a Pyrrolidine Ring

FUJIWARA, Hideki; FUJIWARA, Emiko; KOBAYASHI, Hayao

The molecular conductors and superconductors containing magnetic transition metal anions have been studied for the investigation of the interplay between the conductivity and magnetism. On the other hand, several attempts have been also performed using donors containing a stable TEMPO or NN radical to investigate the interaction between conduction electrons and localized spins of the organic stable radical parts for the development of novel multifunctional materials and ferromagnetic metals. Herein we report the synthesis, structures and physical properties of new TEMPO-containing electron donors in which a TEMPO radical part connects to the EDT-TTF (**1**) or EDO-TTF (**2**) skeletons through a pyrrolidine ring. The ESR spectra of them indicated three absorption lines characteristic of the TEMPO radical. The donors are paramagnetic and showed a slight antiferromagnetic interaction at low temperature region (θ = –2.4 and –3.2 K, respectively). The CV measurement showed two pairs of reversible redox waves originated from the TTF part and one oxidation wave from the TEMPO radical part and indicated the possibility of the coexistence of both the cation-radical and localized spins.

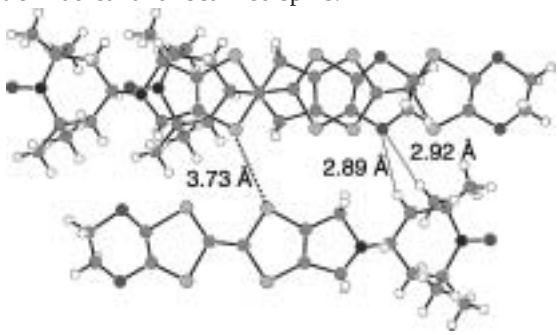

Figure 1. Crystal structure of **2**.

IV-F-4 Synthesis, Structures and Properties of New TTF and TTP Donors Containing a PROXYL Radical

FUJIWARA, Hideki; FUJIWARA, Emiko; KOBAYASHI, Hayao

To investigate the interaction between conduction electrons of the TTF-type donors and localized spins of the organic stable radical parts we have synthesized and studied the molecular conductors containing a stable TEMPO radical so far. Herein we report the synthesis, structures and physical properties of novel TTF (**1a**, **b**) and TTP (**2**) donors containing a PROXYL radical. X-Ray structure analysis of **1** showed that the PROXYL part has a racemic structure and connects to the TTF part in the chair-formed conformation. The ESR spectra of them indicated three absorption lines characteristic of the PROXYL radical. The donors **1a**, **b** are paramagnetic and showed a slight antiferromagnetic interaction at low temperature region (θ = –2.1 and –8.7 K, respectively) and **1b** showed a rapid decrease of magnetic susceptibilities around 5 K, which seems to be originated from an antiferromagnetic transition. The CV measurement of **1a**, **b** showed two pairs of reversible redox waves originated from the TTF part and one oxidation wave from the PROXYL radical part and indicated the possibility of the coexistence of both the cation-radical and localized spins.

Figure 1. Crystal structure of **1a**.

IV-F-5 Syntheses, Structures and Physical Properties of New π-extended TTF Derivatives Containing a Organic Radical

FUJIWARA, Emiko; FUJIWARA, Hideki; KOBAYASHI, Hayao

We have succeeded in the syntheses of several donors **1**–**3** containing TTF moiety and 2,2,5,5-tetramethylpyrrolin-1-yloxyl (radical part) within single-molecules. Crystal structure analysis on a red crystal of the donor **3** revealed that the TTF moiety is almost planar. Electrochemical properties of the donor **1**–**3** were investigated by cyclic voltammetry. All the donors showed four pairs of reversible redox waves (E = 0.58, 0.86, 0.95, 1.67 V for **1**, E = 0.60, 0.85, 0.96, 1.63 V for **2**, E = 0.59, 0.88, 0.96, 1.69 V *vs.* Ag/AgCl in PhCN for **3**). On the other hand the aldehyde of 2,2,5,5-tetramethylpyrrolin-1-yloxyl showed one reversible redox wave (0.98 V) under the identical conditions, suggesting that the third redox process at 0.95–0.96 V occurs at radical part. The ESR spectra of benzene solutions of the donors **1**–**3** were measured to confirm the existence of the NO radical part. All of them showed three absorption lines (g = 2.0059 and a_N = 14.3–14.4 G) characteristic of the NO radical. The static magnetic susceptibilities of the donor **2**–**3** were measured by SQUID magnetometer. Both of them showed Curie-Weiss temperature dependence with slight antiferromagnetic interaction and magnetization corresponding to one S = 1/2 spin per molecule (C = 0.398 K·emu·mol^{-1}, θ = –2.3 K for 2 and C = 0.355 K·emu·mol^{-1}, θ = –0.73 K for **3**). Preparation of cation radical salts of the donor **3**, where TTF moiety and radical part are expected to bear conducting and magnetic properties respectively, was carried out, and they showed semiconducting behavior.

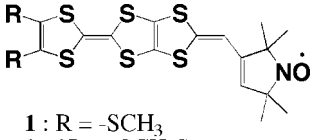

1 : R = -SCH_3
2 : 2R = -SCH_2S-
3 : 2R = -SCH_2CH_2S-

Figure 1. Structure of **1**–**3**.

IV-G Field Effect Transistors with Organic Semiconductors

The mechanism of carrier transport in organic semiconductors and carrier injection from metal electrodes becomes the most important subject to be elucidated for the construction of high performance organic thin film devices. We have studied electrical properties of organic films using field effect transistors.

IV-G-1 Electrical Properties of Phathalocyanine films Prepared by Electrophoretic Deposition

TAKADA, Masaki[1]; YOSHIOKA, Hirokazu[2]; TADA, Hirokazu; MATSUSHIGE, Kazumi[2]
([1]GUAS; [2]Kyoto Univ)

Optical and electrical properties of phthalocyanine (Pc) films have long been studied because of their potential applications to gas sensors, organic light emitting devices and electronic devices including field effect transistors (FETs). Since most Pcs are insoluble in aqueous and organic solvent, Pc films studied so far were prepared by vacuum evaporation technique. We prepared Pc films onto interdigital electrodes by electrophoretic deposition of protonated Pc molecules in the mixture solution of trifluoroacetic acid and dichrolomethane. Contaminations in the films were removed by annealing treatment, and the films exhibited FET behaviors of p-type semiconductors (Figure 1). Carrier mobility, conductivity and carrier density of the films were 1.4×10^{-5} cm^2/Vs, 7.7×10^{-7} S/cm and 6.6×10^{16} cm^{-3}, respectively. These values are almost the same as those of vacuum evaporated films examined so far. It is found that electrophoretic deposition is useful for selective growth of active layers in organic devices.

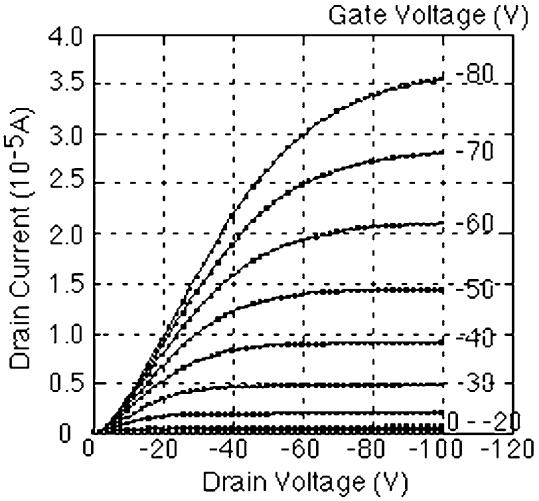

Figure 1.

IV-G-2 Field Effect Transistors with BTQBT Films

TAKADA, Masaki[1]; GRAAF, Harald; YAMASHITA, Yoshiro[2]; TADA, Hirokazu
([1]GUAS, [2]Tokyo Inst. Tech.)

The carrier mobility of organic single crystals are in the range of 1 cm^2/Vs which is comparable to that of amorphous silicon. However, most organic films in devices exhibited the mobility less than 10^{-3} cm^2/Vs due to the existence of grain boundaries. It is thus important to control molecular packing in the films of well-designed molecules. We have choosed BTQBT as the candidate for active layers of field effect transistors (FETs), since the single crystal showed large mobility and highly oriented films were prepared on various substrates. It was found that BTQBT showed p-type semiconducting behavior in air with the mobility of 0.01–0.5 cm^2/Vs, depending on growth conditions.

IV-H Preparation and Characterization of Highly Ordered Molecular Films on Silicon Bound Through Si–C Covalent Bond

Self-assembled monolayers (SAMs) have received considerable attention because of their potential applications to molecular scale electronic devices. Covalently bond alkane SAMs formed by reaction between alkene and hydrogen terminated silicon are of increasing interest as nano-interface for molecular electronics devices fabricated on silicon microstructures. We have studied the growth manner and electronic structure of Si–C junction using scanning probe microscope such as STM (scanning tunneling microscope), AFM (atomic force microscope) and KFM (Kelvin force microscope).

IV-H-1 AFM Studies of Organic Monolayers on Silicon (111) Surfaces

ARA, Masato[1]; GRAAF, Harald; TADA, Hirokazu
([1]GUAS)

Surface morphorogy of SAMs formed by the reaction between 1-dodecene, octadecene and methyl 10-undecenoate and hydrogen terminated silicon (111) surfaces were studied with contact mode AFM. Both p and n type Si(111) surfaces with atomically flat terraces were obtained by chemical etching with NH4F solution. Atomically flat surfaces were also observed in AFM images of SAMs on silicon, indicating that the molecules formed highly-oriented films. We found differences in adhesion force and contact angle depending on the molecules and density of molecules. Electronic structure at the interface will be revealed with KFM studies as well as ultraviolet photoelectron spectroscopy.

IV-I Nanolithography of Organic and Inorganic Materials for Molecular Scale Electronics

Great progress is being made in integration and miniaturization of electronic devices by various techniques of micro- and nano-lithography. Modification of chemical structure of organic compounds with scanning probe microscopes is one of the most promising ways for nano-fabrication. We have studied nano-modification of self-assembled monolayers (SAMs) grown on silicon.

IV-I-1 Microscopic Patterning on the Polysilane Films by the Laser Induced Grating Technique

OKAMOTO, Koichi[1]; TOJO, Tomoaki[1]; TADA, Hirokazu; TERAZIMA, Masahide[1]; MATSUSHIGE, Kazumi[1]
([1]Kyoto Univ.)

[*Mol. Cryst. Liq. Cryst.* in press]

Microscopic patterning on polysilane thin films was observed after photoexcitation with an optical interference pattern using a nanosecond pulsed laser. The patterning processes were monitored by the diffraction of the probe beam. The observed diffraction signals consist of the transient grating component due to the temperature change and the permanent grating component due to a chemical reaction. It was found that the microscopic pattern was destroyed with prolonged laser radiation. The created microscopic pattern was observed by the optical microscope.

IV-I-2 AFM Lithography of Organic Monolayers Bound Covalently on Silicon

ARA, Masato[1]; GRAAF, Harald; TADA, Hirokazu
([1]GUAS)

The alkane monolayer on silicon was degraded by applying a positive bias voltage at the substrate, which resulted in the oxidization of silicon surfaces (Figure 1). The height of the silicon oxide depends on the applied voltage, the width on the curvature radius and the humidity of the atmosphere of the AFM tip. The patterned area is available for different kinds of advanced techniques: 1) covering the oxide with other self-assembled monolayer by trichloro- or trimethoxy siliyl compounds; 2) removing of the silicon oxide by NH_4F-solution and using the established hydrogen terminated silicon for light or heat induced reaction with other alkenes or using the electrical conductive for metal plating; 3) etching of ditches by NH_4F/H_2O_2 solution and fill this ditches with metal by plating.

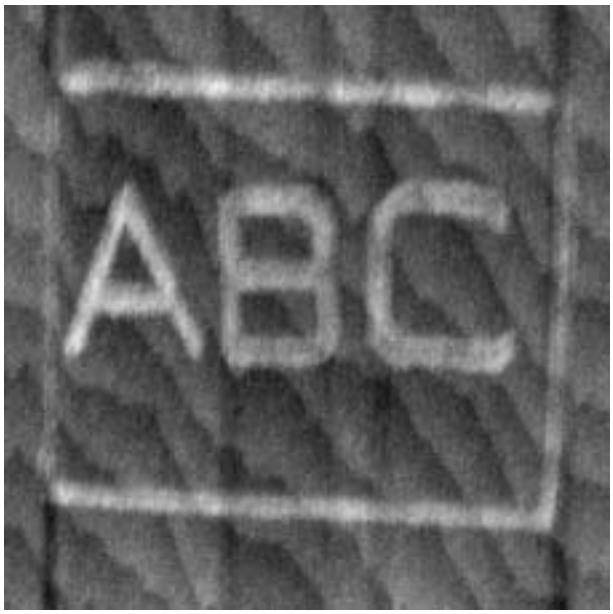

Figure 1.

IV-J Development of New Molecular Conductors

Molecular conductors at the first stage were single component systems where only one degree of freedom governs transport properties. For example, the conduction band in KCP is a one-dimensional d_{z^2} band. TTF-TCNQ has a HOMO band of TTF and a LUMO band of TCNQ, but both of them are one-dimensional pure π bands. Recently, however, increasing number of interesting systems which have "two" bands with different characters near the Fermi level, or where itinerant pπ electrons interact with localized *d* spins, have been reported: for example, the DCNQI-Cu salt with π and itinerant *d*, $Pd(dmit)_2$ salts with a two-dimensional HOMO band and a one-dimensional LUMO band, the organic superconductor $(TMET\text{-}STF)_2BF_4$ with a two-dimensional HOMO band and a one-dimensional HOMO band. On the other hand, in the BETS salt with $FeCl_4$, localized *d* spins on the Fe^{3+} ions interact with itinerant π electrons. Such multi component systems exhibit interesting physical properties derived from the interplay of many degrees of freedom. The aim of this project is to forward further development of molecular-based conductors with many degrees of freedom.

Main subjects are;

(1) Supramolecular organic conductors: Design of the *inter*-molecular interaction is indispensable in the rational development of molecular materials to still higher forms. From this point of view, we are trying to introduce supramolecular chemistry into the molecular conductor. We have a great interest in an iodine-based *halogen bond* as a supramolecular synthon. Carbon-bound iodine atoms are known to act as Lewis-acids and form short contacts with various species which can act as a Lewis-base (for example, –CN, –Cl, –Br, and =S). This non-covalent interaction (halogen bond) can be strong and directional, which would lead to 1) the reliable regulation of the molecular arrangement and orientation, 2) enhancement of an interaction between conduction electrons and functional molecules in the assembly of molecules.

(2) π-*f* system: 4*f* electrons in rare-earth ions exhibit very large anisotropic magnetic moments, as a result of the strong spin-orbit coupling and the high degeneracy due to strong correlation in a well-localized 4*f* orbital. This feature is never observed in 3*d* ions, organic π molecules nor other systems. We are trying to develop molecular conductors where 4*f* electrons are incorporated into a conduction π electron system. Using the heavy rare-earth complex anions $[Ln(NCS)_6]^{3-}$ (Ln = Ho, Er, Yb and Y) and organic donors BO and TTP, we have synthesized the first stable π-*f* metals that remain metallic down to very low temperature.

(3) Two-band system based on transition metal complexes: We have studied $Pd(dmit)_2$ salts with a series of pyramidal cations and found interesting supramolecular interactions through the tellurium-based secondary bond in Me_3Te and Et_2MeTe salts. These compounds demonstrate that the supramolecular interaction provides the system where two different types of Fermi surfaces coexist within the 'same' crystal. This indicates that the tellurium-based secondary bond can be used for the tuning of the molecular arrangement and thus inter-molecular interactions in the anion radical salts.

IV-J-1 Synthesis and Properties of Novel Donor-Type Metal-Dithiolene Complexes Based on 5,6-dihydro-1,4-dioxin-2,3-dithiol (edo) Ligand

WATANABE, Eiji[1]; FUJIWARA, Masahiro[1]; YAMAURA, Jun-ichi[1]; KATO, Reizo
([1]Univ. Tokyo)

[*J. Mater. Chem.* **11**, 2131 (2001)]

The donor-type metal-dithiolene complexes, where the central C=C bond in the TTF-based organic donor is replaced by the transition metal, are promising materials for the formation of molecular metals and superconductors. One drawback in the conventional donor-type metal-dithiolene complexes is their poor-solubility in usual organic solvents which gives a difficult obstacle in the preparation of the cation radical salt with high quality. We have successfully synthesized a novel donor-type metal-dithiolene complex, $Ni(edo)_2$ [edo = 5,6-dihydro-1,4-dioxin-2,3-dithiolate], and its mixed-ligand derivatives. The edo complex is an analog of the organic donor BEDO-TTF (BO) [bis(ethylenedioxo)-tetrathiafulvalene]. The BO molecule shows higher solubility in various organic solvents than other organic donors and is known to provide superconducting cation radical salts. The obtained edo-based complexes exhibit largely improved solubility and their donor abilities have been confirmed. The cation radical salts based on these newly synthesized metal complexes have exhibited novel donor arrangements including the trimer-based κ-type one. Notably the edo ligand shows a unique repulsive inter-ligand interaction and the face-to-face overlap of the edo ligands seems difficult to occur in the crystal, which frequently leads to the twisted and spanning overlap of the metal complexes. This is in contrast to the case of BO-based cation radical salts where the organic donor BO shows a strong tendency to aggregate into a two-dimensional layered structure by the aid of both inter-molecular C–H···O and side-by-side heteroatom contacts. In other words, the edo unit seems to have a strong tendency to restrict the mode of overlap, as the ethylenedioxo unit within BO but in the opposite way. An origin of this unique feature of the edo ligand remains an open question. We would make the most of what the edo ligand provides (improved solubility and unique molecular arrangement) in combination with the extended π-ligands derived from TTF. In such a largely elongated π molecule, its poor solubility is a serious problem and the spanning overlap mode plays an important role in the formation of the three-dimensional electronic structure. Further studies are in progress.

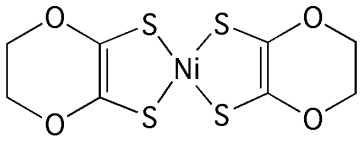

$Ni(edo)_2$

IV-J-2 Structural and Physical Properties of Conducting Cation Radical Salts Containing Supramolecular Assemblies Based on *p*BIB Derivatives (*p*BIB = *p*-Bis(iodoethynyl)benzene)

YAMAMOTO, Hiroshi[1]; MAEDA, Ryoko[2]; YAMAURA, Jun-ichi[2]; KATO, Reizo
([1]RIKEN; [2]Univ. Tokyo)

[*J. Mater. Chem.* **11**, 1034 (2001)]

A cation radical salt $(ET)_3Cl$(*p*BIB) (ET = bis(ethylenedithio)tetrathiafulvalene, *p*BIB = *p*-bis(iodoethynyl)benzene) salt is a unique organic metal containing supramolecular assemblies based on the *p*BIB molecule and the Cl anion, ···Cl···*p*BIB···Cl···. We newly prepared chloride and bromide salts of ET with the use of di- and tetra-substituted *p*BIB derivatives: 1,4-difluoro-2,5-bis(iodoethynyl)benzene (DFBIB), 1,2,4,5-tetrafluoro-3,6-bis(iodoethynyl)-benzene (TFBIB), 1,4-bis(iodoethynyl)-2,5-dimethyl-benzene (BIDMB), and *p*-bis(iodoethynyl)benzene-d_4 (*p*BIB-d_4). The substitution effect has been studied by X-ray structure analyses, tight-binding band calculations, and resistivity measurements. The halide anion replacement ($Br^- \rightarrow Cl^-$) as well as the deuterium and difluoro-substitutions on the *p*BIB molecule do not change the fundamental crystal structure and the metallic behavior but change the $X^-\cdots$*p*BIB$\cdots X^-$ period and the inter-chain distance. These systematic deformations of the anion framework act as *anisotropic chemical pressure* onto the donor layer and lead to a rotation of the donor molecule around the longitudinal molecular axis. The rotation of the donor molecules affects on the inter-molecular overlap integrals of HOMO and the tight-binding calculations indicate that the difluoro- and Cl^--substitutions increase the anisotropy of the Fermi surface. On the other hand, the tetrafluoro- and dimethyl-substitutions induce different donor arrangements that lead to semiconducting behaviors.

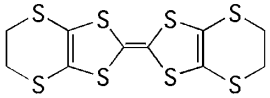

ET

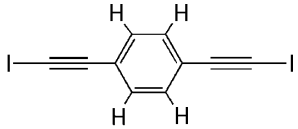

*p*BIB

IV-K Systematic Study of Organic Conductors

Thanks to the systematic view to structure-property relationship studied particularly in BEDT-TTF-based conductors, recently our understanding of organic conductors has made a great progress. We have investigated charge ordered phases of molecular conductors, and have shown what kinds of charge ordered patterns are stable depending on the crystal structures. We have extended our molecular-orbital-calculation-based estimation of intermolecular interactions in organic conductors to πd-systems containing magnetic anions, and have discussed magnetic interactions *J* from the orbital overlaps. From the concept of "universal phase diagram" in the θ-phase, we can predict metal-insulator transition temperatures of a large number of organic conductors. We have applied this rule to tetrathiapentalene (TTP) compounds, verifying that this rule holds to these compounds with some shift of the metal-insulator boundary owing to the small *U*. We have prepared selenium containing TTP compounds, which have shown lower transition temperatures than the sulfur analogs. We also have shown that substitution of TTP donors with long alkyl chains such as ethylthio groups leads to preferable crystal structures, improving the balance of soft terminal parts and the extended core part of the long TTP molecules.

IV-K-1 Estimation of Off-Site Coulomb Integrals and Phase Diagrams of Charge Ordered States in the θ-Phase Organic Conductors

MORI, Takehiko
(Tokyo Inst. Tech. and IMS)

[*Bull. Chem. Soc. Jpn.* **73**, 2243 (2000)]

Intermolecular Coulomb repulsion, *V*, of the highest occupied molecular orbitals (HOMO) of BEDT-TTF (bis(ethylenedithio)tetrathiafulvalene) is calculated for various molecular geometries. The bare *V* is a quantity that is easily estimated under the point charge approximation. As far as the screened *V* in actual crystals is proportional to the calculated bare *V*, the usual θ-phase prefers the horizontal or diagonal stripe, whereas the vertical stripe becomes comparatively stable in the limit of the small dihedral angle (in the metallic limit) (Figure 1). The phase diagrams of the θ-phase are discussed under the combination of the static charge distribution (the atomic limit) and the Stoner model (the extended Stoner model). The model contains two order parameters: the spin polarization, S_z, and the charge order, n-1/2. This model explains why the insulating state of the Rb salt below 190 K is a paramagnetic charge-ordered state, while the Cs salt has a different insulating phase below 20 K. The lattice dimerization of the Rb salt can be explained only from *V*.

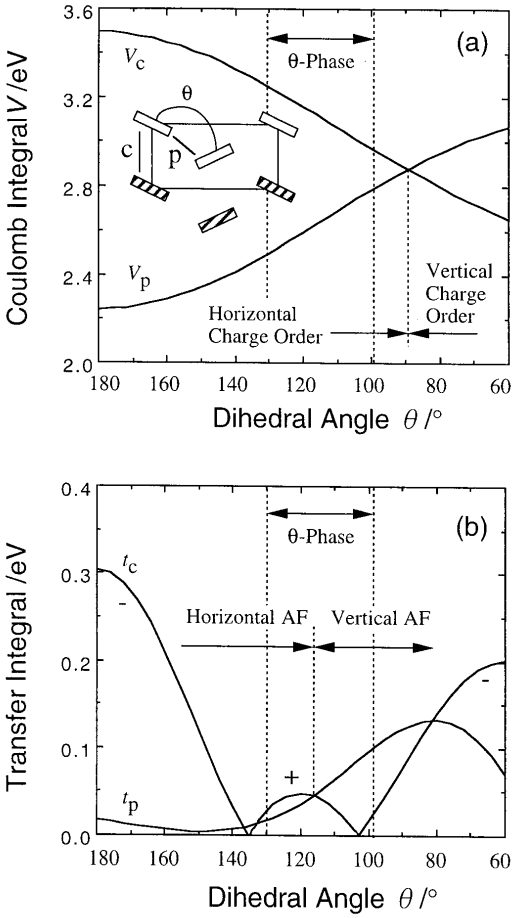

Figure 1. (a) Intermolecular Coulomb integrals, *V*, and (b) transfer integrals, *t*, between HOMO of two tilted BEDT-TTF molecules, calculated as a function of the dihedral angle, θ, in the θ-phase.

IV-K-2 Estimation of π-d Interactions in Organic Conductors Including Magnetic Anions

MORI, Takehiko[1]; KATSUHARA, Mao[2]
([1]Tokyo Inst. Tech. and IMS; [2]Tokyo Inst. Tech.)

Magnetic interactions in organic conductors including magnetic anions, such as λ-$(BETS)_2FeCl_4$ and κ-$(BETS)_2FeCl_4$ [X = Cl and Br], are estimated from the intermolecular overlap integrals: the overlaps

between anions for J_{dd}, and those between anions and donors for $J_{\pi d}$. From this, the most stable spin alignments are decided, and such quantities as the Neel and Weiss temperatures, as well as the magnitude of spin polarization on the π-molecules are evaluated on the basis of the mean-field theory of πd-systems. The calculation is extended to several other πd-conductors, which are classified depending on the magnitudes of the direct dd- and indirect πd-interactions (Figure 1).

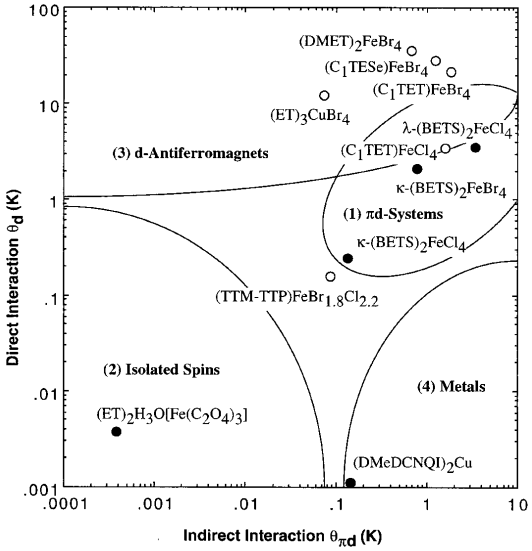

Figure 1. Calculated contributions of direct and indirect interactions to the Weiss temperatures. The closed circles designate metallic compounds at low temperatures.

IV-K-3 Tetrathiapentalene Derivatives with Long Alkyl Chains

KIMURA, Shinya[1]; KURAI, Hiroyuki[1]; MORI, Takehiko[2]; MORI, Hatsumi[3]; S. TANAKA, Shyoji[3]
([1]Tokyo Inst. Tech.; [2]Tokyo Inst. Tech. and IMS; [3]ISTEC)

[*Bull. Chem. Soc. Jpn.* **74**, 59 (2001)]

Bis-fused π-electron donors having alkylthio chains, C$_n$TET-TTP (2-[4,5-bis(alkylthio)-1,3-dithiol-2-ylidene]-5-(4,5-ethylenedithio-1,3-dithiol-2-ylidene)-1,3,4,6-tetrathiapentalene; n = 2–4) have been synthesized. C$_2$TET-TTP (**1a**) forms radical-cation salts with BF_4^- and ClO_4^-, which are metallic (σ_{rt} = 900–2500 Scm^{-1}) down to helium temperatures. The I_3 salts of C$_3$TET-TTP (**1b**) and C$_4$TET-TTP (**1c**) are semiconductive from room temperature (σ_{rt} = 0.04 and 0.025 Scm^{-1}, respectively). (C$_2$TET-TTP)$_2$ClO$_4$ has uniform stacks of the donors, and has an elliptical Fermi surface characteristic of two-dimensional metals. (C$_4$TET-TTP)I_3 is dimeric, and can be regarded as a band insulator. These crystal structures demonstrate the tendency that the long alkyl chains increase the anion content, and stabilize the usual stacking structure as well as the dimerization.

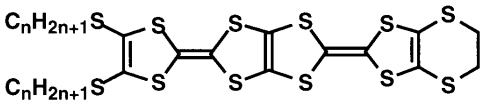

C$_n$TET-TTP **1a** n = 2
1b n = 3
1c n = 4

IV-K-4 TCNQ Complex with θ-Type Donor Arrangement: (TMET-TS-TTP)$_2$(TCNQ)

ARAGAKI, Masanobu[1]; HOSHINO, Hirotada[1]; MORI, Takehiko[2]; MISAKI, Yohji[3]; TANAKA, Kazuyoshi[3]; MORI, Hatsumi[4]; S. TANAKA, Shyoji[4]
([1]Tokyo Inst. Tech.; [2]Tokyo Inst. Tech. and IMS; [3]Kyoto Univ.; [4]ISTEC)

[*Adv. Mater.* **12**, 983 (2000)]

A new tetrathiapentalene donor with selenium atoms, TMET-TS-TTP is prepared. (TMET-TS-TTP)$_2$-(TCNQ) has θ-type donor arrangement with a comparatively small dihedral angle (118°), and TCNQ acts as an isolated anion. This complex undergoes a metal insulator transition at 120 K accompanied by the broadening of the ESR intensity, suggesting an antiferromagnetic order.

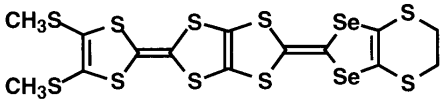

TMET-TS-TTP

IV-K-5 Universal Phase Diagram of θ-Type TMET-TTP Salts

ARAGAKI, Masanobu[1]; HOSHINO, Hirotada[1]; MORI, Takehiko[2]
([1]Tokyo Inst. Tech.; [2]Tokyo Inst. Tech. and IMS)

[*J. Phys. Soc. Jpn.* **70**, 1642 (2001)]

A new θ-type TMET-TTP salt (TMET-TTP)$_2$HSO$_4$, which has smaller dihedral angle (116°), and has 2:1 composition, is prepared. This salt undergoes a metal insulator transition at around 100 K. The ESR measurement indicates that the low-temperature insulating state is paramagnetic. Thanks to this exceptional salt, a universal phase diagram of θ-type TTP salts can be discussed similarly to θ-type ET salts. In the θ-type ET salts, the universal phase diagram holds in the uniform quarter-filled band. However, our works in the θ-type TMET-TTP salts prove that the universal phase diagram is not largely influenced by the band-filling and the position of the Fermi energy.

IV-K-6 Selenium Analogs of Tetrathiapentalene Derivatives with Long Alkyl Chains

ARAGAKI, Masanobu[1]; KIMURA, Shinya[1]; KATSUHARA, Mao[1]; KURAI, Hiroyuki[1]; MORI, Takehiko[2]
([1]Tokyo Inst. Tech.; [2]Tokyo Inst. Tech. and IMS)

[*Bull. Chem. Soc. Jpn.* **74**, 833 (2001)]

A novel selenium-containing bis-fused tetrathiafulvalene donor, C_2TET-TS-TTP (2-[4,5-bis(ethylthio)-1,3-dithiol-2-ylidene]-5-(4,5-ethylenedithio-1,3-dithiol-2-ylidene)-1,3,4,6-tetrathiapentalene) has been synthesized. The ClO_4^-, BF_4^-, and PF_6^- salts of C_2TET-TS-TTP are isostructural, having β-type structures. These salts are essentially metallic down to low temperatures.

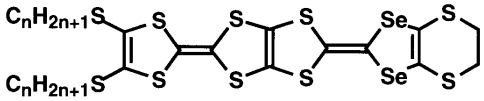

C_2TET-TS-TTP

IV-K-7 1:1 Composition Organic Metal Including a Magnetic Counteranion, (TTM-TTP)$FeBr_{1.8}Cl_{2.2}$

KATSUHARA, Mao[1]; ARAGAKI, Masanobu[1]; MORI, Takehiko[2]; MISAKI, Yohji[3]; TANAKA, Kazuyoshi[3]
([1]Tokyo Inst. Tech.; [2]Tokyo Inst. Tech. and IMS; [3]Kyoto Univ.)

[*Chem. Mater.* **12**, 3186 (2000)]

An organic donor, TTM-TTP forms 1:1 donor/anion salts with $FeCl_4^-$ and $FeBr_4$, (TTM-TTP)$FeX_4(PhCl)_{0.5}$ (X = Cl and Br), which have one-dimensional dimerized columns and are insulators even at room temperature. In contrast, the salt with an alloyed anion, (TTM-TTP)$FeBr_{1.8}Cl_{2.2}$, shows high electrical conductivity of about 1000 Scm^{-1} at room temperature and remains metallic down to 160 K. This salt has uniform, one-dimensional, donor columns. This is the first 1:1 donor/anion composition organic metal with a magnetic counteranion. These compounds exhibit weak magnetic interactions; the Weiss temperatures are around 1–3 K.

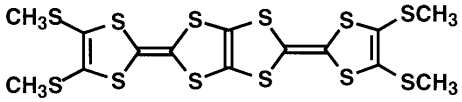

TTM-TTP

IV-K-8 Marginal Paramagnetic State of a One-Dimensional Half-Filled Alternating Chain in (TTM-TTP)AuI_2

KAWAMOTO, Tadashi[1]; MORI, Takehiko[2]; YAMAMOTO, Takashi[3]; TAJIMA, Hiroyuki[3]; MISAKI, Yohji[4]; TANAKA, Kazuyoshi[4]
([1]Tokyo Inst. Tech.; [2]Tokyo Inst. Tech. and IMS; [3]ISSP, Univ. Tokyo; [4]Kyoto Univ.)

[*J. Phys. Soc. Jpn.* **69**, 4066 (2000)]

(TTM-TTP)AuI_2 has a dimerized structure along the donor stacking direction, and shows semiconducting behavior below room temperature. ESR, static magnetic susceptibility, and optical reflectance of this salt have been measured to investigate the spin state and the electronic correlation. The ESR signal has been observed from room temperature to 3 K, and the spin susceptibility shows paramagnetic behavior with a rapid decrease below 10 K. The static magnetic susceptibility is paramagnetic and has an anomaly around 10 K in agreement with the ESR result. The chain axis optical reflectance spectra show clear optical gap in the mid-infrared region. An attempt is undertaken to analyze the optical spectrum by means of the one-dimensional dimerized Hubbard model, which suggests that the on-site Coulomb repulsion, *U*, is small and the spin polarization is located at the marginal paramagnetic boundary. These results indicate that this compound is not a band-insulator but the Mott insulator with a small spin gap.

IV-L Organic Synthesis for Molecular Electronic Devices

The mechanism of electronic conduction through a single molecule is quite different from that of the bulk organic conductive materials. In the latter the charges are carried by soliton, however in the former theories predict that the conduction generally involves tunneling or a resonant tunneling mechanism. A few experiments support the prediction, however there is neither systematic experimental studies nor established theory for single molecular conduction. We use (1) scanning probe microscopic (SPM) technique in ultra high vacuum, and (2) planner nano-gap electrodes for the measurements. Design of the target organic molecules and the measurement system is important for reliable results. We have been preparing (1) self standing organic molecules for measurement by SPM, (2) photo-responsible molecular wires, (3) long molecular wires with low Eg which can be observed optically on nano-gap electrodes. Conduction of gold nano-particles / organic dithiols composite system is also studied.

IV-L-1 "N-Fused Porphyrin": A New Tetrapyrrolic Porphyrinoid with A Fused Tri-Pentacyclic Ring

FURUTA, Hiroyuki[1,3]; ISHIZUKA, Tomoya[1]; OSUKA, Atsuhiro[1]; OGAWA, Takuji[2,3,4]
([1]Kyoto Univ.; [2]Ehime Univ.; [3]JST; [4]IMS)

[*J. Am. Chem. Soc.* **122**, 5748 (2000)]

The syntheses and X-ray structures of novel porphyrinoids, "N-fused porphyrins (NFPs)," and their reactivity were described. NFP was spontaneously produced from the bromo-substituted N-confused tetraarylporphyrin in a pyridine solution at room temperature. X-ray diffraction analyses revealed that the porphyrinoid core containing a fused tri-pentacyclic ring is almost planar. The deviation from the mean plane of 4e¢, for example, was within 0.30 Å. The peripheral aryl substituents were tilted 50.4, 53.5, 64.4, and 12.4° relative to the porphyrin mean plane, respectively. The occurrence of a three-centered hydrogen bonding in the NFP core was inferred by the downfield shift of the inner NH signal (*e.g.*, 8.48 ppm for 4e¢) in 1 H NMR and the short distances (within 2.4–2.9 Å) among the inner core nitrogens, N2,N3, and N4. The optical absorption spectra of NFPs exhibit Soret-like transitions around 360, 500, and 550 nm and weak Q-like bands around 650, 700, 850, and 940 nm in CH_2Cl_2. The electrode process of 4e¢ showed the first oxidation at 0.08 V and reduction at –1.37 V (*vs.* Fc/Fc+), which suggested the small energy gap attributed to the unusual long-wavelength absorption was mainly due to the rising of the HOMO energy level. The first-order rate constants (kf) for the transformation from NCPs to NFPs were largely affected by the substituents at the meso position, showing a good correlation with Hammet ó + parameters. Moreover, the reverse reaction from NFPs to NCPs was observed in the CH_2Cl_2 solution by treating with a base. Dynamic ring inversion in the tetrapyrrolic porphyrin core is discussed.

IV-L-2 Chemical Approach Toward Molecular Electronic Device

OGAWA, Takuji[1,2,3]; KOBAYASHI, Keijiro[2]; MASUDA, Go[2]; TAKASE, Takuya[2]; SHIMIZU, Yuusuke[2]; MAEDA, Seisuke[2]
([1]JST; [2]Ehime Univ.; [3]IMS)

[*Trans. Mater. Res. Soc. Jpn.* **26**, 733 (2001)]

An attempt to actualize high-speed information processing system with molecular electronic devices is a fascinating approach within several other possible ideas for practical use of organic molecules for electronic devices. In order to fabricate the high-speed molecular electronic device, we need molecules of sub-micrometer size with rigid structure and high functionality. We have prepared several "molecular wires" based on porphyrin and related compounds, and studied their electronic properties by using gold nano particles and gold nano-gap electrodes.

IV-L-3 Prospects and Problems of Single Molecule Information Devices

WADA, Yasuo[1]; TSUKADA, Masaru[2]; FUJIHIRA, Masamichi[3]; MATSUSHIGE, Kazumi[4]; OGAWA, Takuji[5,7]; HAGA, Masa-aki[6]; TANAKA, Shoji[7]
([1]Hitachi Co.; [2]Univ. Tokyo; [3]Tokyo Inst. Tech.; [4]Kyoto Univ.; [5]Ehime Univ.; [6]Chuo Univ.; [7]IMS)

[*Jpn. J. Appl. Phys.* **39**, 3835 (2000)]

Current information technologies use semiconductor devices and magnetic/optical discs, however, it is foreseen that they will all face fundamental limitation within a decade. This paper reviews the prospects and problems of single molecule devices, including switching devices, wires, nanotubes, optical devices, storage devices and sensing devices for future information technologies and other advanced application in the next paradigm. The operation principles of these devices are based on the phenomena occurring within a single molecule, such as single electron transfer, direct electron-hole recombination, magnetic/charge storage and legand-receptor reaction. Four possible milestones for realizing the Peta(10^{15})-floating operations per second (P-FLOPS) personal molecular supercomputer are described, and the necessary technologies are listed. These include, (1) two terminal conductance measurements on single molecule, (2) demonstration of two terminal molecular device characteristics, (3) verification of three terminal molecular device characteristics and (4) integration of the functions of "molecular super chip." Thus, 1000 times higher performance information technologies would be realized with molecular device.

IV-L-4 Synthesis and Characterization of N-Confused Porphyrinatoantimony(V): Toward Low Energy Gap Molecular Wire

OGAWA, Takuji[1,2,3]; FURUTA, Hiroyuki[4]; MORINO, Ayako[2]; TAKAHASHI, Minako[2]; UNO, Hidemitsu[2]
([1]JST; [2]Ehime Univ.; [3]IMS; [4]Kyoto Univ.)

[*J. Organomet. Chem.* 551 (2000)]

N-Confused tetraarylporphyrinatoantimony(V) dimethoxides were synthesized, and their X-ray crystallographic structure, absorption spectra and voltammetric spectra were studied. X-ray crystallographic structure revealed neutral molecules with no counter anion. From the absorption spectra and voltammetric studies we estimated their energy gaps to be about 0.2 eV less than the corresponding porphyrinatoantimony(V). The axial ligands could easily be exchanged in solvent alcohol by acid promotion. These characteristics of N-confused porphyrinatoantimony(V) indicate that they are good candidates for the molecular wire component.

IV-L-5 N-Confused Double-Decker Porphyrins

FURUTA, Hiroyuki[1,3]; KUBO, Naoko[1]; MAEDA, Hiromitsu[1]; ISHIZUKA, Tomoya[1]; OSUKA, Atsuhiro[1]; NANAMI, Hideki[2]; OGAWA, Takuji[2,3,4]
([1]Kyoto Univ.; [2]Ehime Univ.; [3]JST; [4]IMS)

[*Inorg. Chem.* **39**, 5424 (2000)]

IV-L-6 Electronic Conductive Characteristics of Devices Fabricated With 1,10-Decanedithiol And Gold Nano Particles Between 1000 nm Electrode Gaps

OGAWA, Takuji[1,2,3]; KOBAYASHI, Keijiro[2]; MASUDA, Go[2]; TAKASE, Takuya[2]; MAEDA, Seisuke[2]
([1]JST; [2]Ehime Univ.; [3]IMS)

[*Thin Solid Films* **393**, 374 (2001)]

Electronic conductive characteristics of composite made from 1,10-decanedithiol and gold nano particles were studied with the pressed pellet and with the devices made from organic dithiols, gold nano particles and *ca.* 1 μm gap gold electrode. The I-V curve of the former pellet was ohmic and the temperature dependence (log(σ)-1/T) of the conductance was not linear. In contrast with it, the micro-gap device exhibited sigmoidal I-V curve. The activation energy for the latter was 6×10^{-3} eV that was one order smaller than the former pellet of 4×10^{-2} eV.

IV-L-7 Synthesis and Characterization of Photo-responsive Molecular Wires Based on Ruthenium Complex Moiety and Thiol Groups

OGAWA, Takuji[1,2,3]; KOBAYASHI, Keijiro[2]; MASUDA, Go[2]; SHIMIZU, Yuusuke[2]
([1]JST; [2]Ehime Univ.; [3]IMS)

[Submitted]

Molecular wires with a ruthenium complex moiety and thiol group precursors for connecting to gold electrodes were synthesized, and their optical and electrochemical properties were investigated. An electronic device was fabricated with one of the ruthenium complexes bearing two thiol groups using 2 nm gold nano-particles as connecting bond on 1-_m-gapped gold electrodes to show that the device had a sharp photo-response.

IV-M Photoelectron Spectroscopy of Organic Solids in Vacuum Ultraviolet Region

IV-M-1 Calculation of Photoelectron Angular Distributions from ω-(n-pyrrolyl)alkanethiol Self-Assembled Monolayers for Different Molecular Orbitals of Pyrrole Group

HASEGAWA, Shinji; YAKUSHI, Kyuya; INOKUCHI, Hiroo; OKUDAIRA K., Koji[1]; UENO, Nobuo[1]; SEKI, Kazuhiko[2]; MORIKAWA, Eizi[3]
([1]Chiba Univ.; [2]RCMS, Nagoya Univ.; [3]Louisiana State Univ. CAMD)

[*Mol. Cryst. Liq. Cryst.* in press]

We calculated photoelectron angular distributions from ω-(n-pyrrolyl)alkanethiol self-assembled monolayers (pyrrolyl-SAMs) for different π molecular orbitals, π_N and π_C, originating from the pyrrole group. The calculations were carried out within a single-scattering approximation of photoemission process. In the approximation, the photoelectron intensity is caused by not only the self-scattering waves from a pyrrole group but also the single-scattering waves scattered in the vicinity of the pyrrole group. Therefore, the angular patterns involve information on the surface arrangement of the pyrrole groups as well as the character of the molecular orbitals.

IV-M-2 Calculated Photoelectron Angular Distributions of ω-(n-pyrrolyl)alkanethiol Self-Assembled Monolayers for Distinction between Different Arrangements of Pyrrole Groups

HASEGAWA, Shinji; YAKUSHI, Kyuya; INOKUCHI, Hiroo; OKUDAIRA K., Koji[1]; UENO, Nobuo[1]; SEKI, Kazuhiko[2]; MORIKAWA, Eizi[3]; SAILE, Volker[3]
([1]Chiba Univ.; [2]RCMS, Nagoya Univ.; [3]Louisiana State Univ. CAMD)

[*J. Electron Spectrosc. Relat. Phenom.* in press]

Photoelectron angular distributions from ω-(n-pyrrolyl)alkanethiol self-assembled monolayers (SAMs) were calculated within a single-scattering approximation of photoemission process. The calculations were carried out on two different surface structures with face-stacked and herringbone arrangements of the pyrrole groups which were deduced from molecular dynamics calculations. The characteristic angular patterns calculated for the molecular orbital originating from the pyrrole group involve information on the orientations of the pyrrole groups, which allows the distinction between these arrangements. The photoelectron angular distributions from the substituted SAMs can be used as a clue for studying the surface structures of the substituent groups.